CENTRO DE INVESTIGACIÓN Y DE ESTUDIOS AVANZADOS DEL INSTITUTO POLITÉCNICO NACIONAL

UNIDAD MÉRIDA

DEPARTAMENTO DE FÍSICA APLICADA

Physicochemical analysis of growth of ZnS thin films synthesized by chemical bath technique from 25°C to 55°C

A dissertation presented by

Irving Josué González Chan

to obtain the degree of

Doctor of Science

in

Physical Chemistry

Advisor

Dr. Andrés Iván Oliva Arias

Merida, Yucatan, Mexico **August 2017**

CENTRO DE INVESTIGACIÓN Y DE ESTUDIOS AVANZADOS DEL INSTITUTO POLITÉCNICO NACIONAL

UNIDAD MÉRIDA

DEPARTAMENTO DE FÍSICA APLICADA

Análisis fisicoquímico del crecimiento de películas delgadas de ZnS sintetizadas por la técnica de baño químico entre 25 °C y 55 °C

Tesis que presenta

Irving Josué González Chan

Para obtener el grado de

Doctor en Ciencias

en

Fisicoquímica

Director de tesis

Dr. Andrés Iván Oliva Arias

Mérida, Yucatán, México. Agosto 2017

Guadalupe, David, Anahí, Mois and Marco
This is for you

ACKNOWLEDGMENTS

To the **Consejo Nacional de Ciencia y Tecnología (CONACYT)** for the scholarship given for my doctoral studies.

To **Dr. Andrés Iván Oliva Arias** for his advice, direction, trust, and support that he gave me in the accomplishment of this work.

To **Dra. Milenis Acosta, Dr. Rodrigo Patiño, Dr. Máximo Pech, and Dr. Geonel Rodríguez** for their valuable comments and suggestions that enriched this work.

To **Ing. Emilio Corona Hernández** for the instrumental contributions that facilitated me the execution of this work.

To technicians **M.C. Mauricio Romero López, M.C. Daniel Aguilar Treviño, M.C. Dora Huerta Quintanilla,** and **Ing. Wilian Javier Cauich Ruiz** for their advices and help with the different characterization techniques used in this work.

To the academic and administrative staff of the Applied Physics Department, especially to **Lourdes Pinelo Rivera** and **Zhirnay Rodríguez Pinelo** for their support with administrative procedures.

To my **colleagues in the Microscopy Laboratory,** for their friendship and support.

CONTENT

LIST OF FIGURES

LIST OF TABLES

ABSTRACT

A physicochemical analysis was performed for a chemical bath where solubility curves and species distribution diagrams were used to obtain the best conditions for zinc sulfide (ZnS) deposition in a range of temperatures between 25 °C and 55 °C. Solubility curves evidenced the necessity to adjust the thiourea concentration for each bath temperature in order to obtain enough amounts of sulfur ions needed for ZnS formation. ZnS thin films were deposited by the chemical bath deposition (CBD) technique at near ambient temperatures from zinc chloride, potassium hydroxide, ammonium nitrate and thiourea solutions. The thiourea concentrations were fixed at 0.7 M (55 °C), 0.95 M (47 °C), 1.25 M (40 °C), 1.7 M (32 °C) and 2.25 M (25 °C) to obtain high quality films. The effects of the bath temperature and deposition time on the dynamic evolution of the ZnS formation were investigated by means of a kinetic study. Higher thickness and rates of growth were observed for increased temperatures. Species distribution diagrams were elaborated from the experimental conditions and suggest that the growth mechanism contains HS^- ions on the part of sulfur species as well as $Zn(OH)_4^{2-}$ and $Zn(OH)_3^-$ ions as complexing species of zinc. An estimated activation energy of 127 ± 5 kJ/mol and the obtained value of 1.03 ± 0.05 as the order of reaction, with thiourea dependence, suggested that the growing mechanism is a chemical process where the formation and absorption of $Zn(OH)_2$ in substrate is involved, to subsequently carry out an exchange reaction between OH^- and HS^- ions.

Chemical, structural, morphological and optical characterizations of the deposited ZnS thin films are reported. The formation of the ZnS or $Zn(OH)_2$ compounds, was identified by X-ray photoelectron spectroscopy (XPS) analysis. The stoichiometric Zn/S molar ratio of the ZnS films increased with the rise of the temperature from 0.367 (25 °C) to 0.906 (55 °C).

X-ray diffraction (XRD) results show amorphous structures for almost all the films, except for the ZnS samples prepared at 47°C and 55°C by using proper concentrations of thiourea, where a preferential cubic phase (111) structure (sphalerite) was identified. Optical characterizations showed a transmittance greater than 80% for wavelengths above 500 nm of the electromagnetic spectrum. The calculated bandgap energy of the ZnS samples is in a range from 3.5 to 3.8 eV when the appropriate thiourea conditions are used, meanwhile for the non-proper conditions this range is reduced between 3.2 and 3.6 eV as a consequence of contamination with $Zn(OH)_2$ in the samples. These characteristics, together with the homogeneous and agglomerates-free surface of the samples, suggest that the obtained ZnS films can be useful for solar cells applications.

RESUMEN

Se llevó al cabo un análisis fisicoquímico de una solución del baño químico donde se utilizaron las curvas de solubilidad y los diagramas de distribución de especies para obtener las mejores condiciones para el depósito del ZnS en un rango de temperaturas entre 25 °C y 55 °C. Las curvas de solubilidad evidenciaron la necesidad de ajustar la concentración de la tiourea para cada temperatura del baño con la finalidad de tener la cantidad suficiente de iones de azufre necesarios para la formación del ZnS. Se depositaron películas delgadas de sulfuro de zinc (ZnS) por la técnica de baño químico a temperaturas cercanas a la del ambiente por medio de una solución que contiene cloruro de zinc, hidróxido de potasio, nitrato de amonio y tiourea. Las concentraciones de la tiourea fueron ajustadas a 0.7 M (55 °C), 0.95 M (47 °C), 1.25 M (40 °C), 1.7 M (32 °C) y 2.25 (25 °C) para depositar películas delgadas de ZnS con alta calidad. Por medio de un estudio cinético, se investigaron los efectos de la temperatura y el tiempo de depósito en la evolución dinámica de la formación del ZnS. Mayores espesores y altas velocidades de crecimiento fueron observados para las mayores temperaturas. Los diagramas de distribución de especies fueron elaborados con las condiciones experimentales y sugirieron que el mecanismo de crecimiento contiene a los iones HS^- por parte del azufre y los iones $Zn(OH)_4^{2-}$ y $Zn(OH)_3^-$ como especies complejantes del zinc. La energía de activación estimada en 127 ± 5 kJ/mol y el orden de la reacción de 1.03 ± 0.05, dependiente de la concentración de la tiourea, sugieren que el mecanismo de crecimiento es un proceso químico en donde interviene la formación y adsorción de $Zn(OH)_2$ y subsecuentemente una reacción de intercambio entre los iones HS^- y OH^-.

Se reportan los resultados de las caracterizaciones química, estructural, morfológica y óptica de las muestras depositadas bajo las diferentes condiciones sugeridas. Usando

espectroscopía de rayos x de fotoelectrones se identificó la formación de ZnS y/o $Zn(OH)_2$ en las películas. El cociente molar estequiométrico Zn/S aumenta con el incremento de la temperatura de 0.367 (25 °C) a 0.906 (55 °C). Los resultados de la difracción de rayos X muestran que la mayoría de las estructuras cristalinas son amorfas, excepto las de las muestras depositadas a 47 °C y 55 °C usando concentraciones apropiadas de tiourea, con un pico de difracción preferencial (111) perteneciente a la estructura cúbica esfalerita. La caracterización óptica mostró una transmitancia mayor a 80 % para longitudes de onda por arriba de los 500 nm del espectro electromagnético. La energía de banda prohibida de las muestras se determinó entre 3.5 y 3.8 eV cuando se usan condiciones apropiadas de tiourea; mientras que para las muestras depositadas en condiciones no apropiadas, este intervalo se reduce entre 3.2 y 3.6 eV como consecuencia de la contaminación de $Zn(OH)_2$ en las muestras. Estas características, en conjunto con la superficie homogénea y libre de aglomerados, hacen que las muestras de ZnS obtenidas sean apropiadas para su aplicación en celdas solares.

PREFACE

Nowadays, the use of renewable energies has gone from being an alternative to a necessity. The inevitable depletion of fossil fuels, the high pollution rates and the effects of global warming are factors that have accelerated the research and implementation of renewable energies. Wind, hydro, geothermal and solar energy are some of these renewable energies that can be available in our world. However, the solar energy stands out among them because its inexhaustible source provided by the sun. The solar energy is converted into thermal or electrical energy. This energy can have a variety of uses, including for generating electricity, providing light, and heating water for domestic, commercial, or industrial uses. There are different ways to capture the solar energy: photovoltaics, solar heating & cooling, concentrating solar power, and passive solar.

The first three are *active* solar systems, which use mechanical or electrical devices that convert the sun's heat or light to another form of useful energy. *Passive* solar buildings are designed and oriented to collect, store, and distribute the heat from sunlight to maintain the comfort of the occupants without the use of moving parts or electronics.

The solar cell is a device that converts the energy coming from the Sun into electrical energy. This conversion can be carried out directly by the photoelectric effect or indirectly by transforming the solar energy into heat or chemical energy. There are three basic types of solar cell. Monocrystalline cells are cut from a silicon ingot grown from a single large crystal of silicon whilst polycrystalline cells are cut from an ingot made up of many smaller crystals. The third type is the thin-film solar cell, which are formed by layers of different materials, deposited in a specific order. Each layer performs a specific function within the working scheme for the conversion of solar energy into electrical energy. The major interest in this

technological application is the possibility to reduce costs of production given that many of the techniques used in the laboratory for depositing the films are versatile and can be implemented at industrial level. Similarly, the cost of the used materials is reduced in comparison to the current silicon-based solar cell technology.

Two types of solar cells based on thin-layer technology have now dawned due to the high efficiencies obtained in the laboratory: the CdTe/CdS and the CuInGaSe (CIGS) solar cells. Both types of solar cells present great potential because of their high efficiency due to the variable and controlled bandgap energy that can be obtained through their composition. The bandgap energy maximizes the absorption of the solar spectrum which provides the highest absorption coefficient within the thin film technology, allowing about 99% of the photons to be absorbed and subsequently used for electrical energy conversion. At laboratory, an efficiency for this type of solar cell of 16% has been reported. Both types of solar cells have in common the use of cadmium sulfide (CdS) as optical window. However, the CdS presents two important limitations: by its nature, it has some degree of toxicity, and below 520 nm of wavelength it presents high absorbance, which means that an important part of the visible spectrum is not captured for conversion. A material with better physical properties for replacing the CdS as optical window in the solar cells is the zinc sulfide (ZnS). This material is practically transparent for all the solar spectrum, allowing to capture all the range of the visible spectrum. Preliminary efforts have shown the use of ZnS as optical window to obtain high efficiencies as 18.6% in the CIGS solar cells. A technique for preparing ZnS films that stands out by its simple implementation and low cost is the chemical bath deposition (CBD); however, a disadvantage in most of the previous works about ZnS preparation is the bath temperatures above 60 °C, leaving room temperatures (~25 °C) practically unexplored. The deposition of ZnS films at temperatures close room conditions becomes an issue of interest

for the industry due to the high potential of scalability, simplification of the fabrication process, and the reduced energy requirements.

The purpose of this work is to contribute for understanding the complex formation equilibria and kinetics of the deposition of the ZnS thin films at temperatures from 25 to 55 °C. The thesis is divided into five chapters. In the first Chapter, an introduction to the CBD technique is presented, highlighting the involved theory for obtaining thin films. Additionally, a brief review of the ZnS material is presented providing its properties, applications and previous investigations made by other authors. Chapter 2 presents the physicochemical analysis performed on the deposition solution from which the solubility curves and the species distribution diagrams are important tools used for determining the best growth conditions for ZnS preparation at temperatures from 25 °C to 55 °C. In Chapter 3, the methodology for preparing the film samples is presented with the conditions established from the physicochemical analysis, as well as the characterization techniques used in this work for obtaining the morphological, chemical, structural and optical properties of the samples. In Chapter 4, a kinetic analysis is proposed for explaining the growing mechanism of the ZnS material. The activation energy of the system is determined as well as the reaction order dependent on the concentration of the thiourea. Finally, in Chapter 5, the results of the morphological, chemical, structural and optical properties of the different samples, obtained with proper and no-proper conditions for deposition, are discussed and compared.

OBJECTIVES

GENERAL

To study the synthesis of zinc sulfide by the chemical bath deposition technique at temperatures from 25 °C to 55 °C in order to determine the best chemical parameters for depositing ZnS thin films with high quality and controlled properties.

SPECIFIC OBJECTIVES

1. To conduct a physicochemical analysis of the chemical solution to obtain the solubility curves and the species distribution diagrams that lead to the proper concentrations of the chemical reagents at room temperature (25 °C).
2. To establish experimental conditions for controlled deposition of ZnS thin films with proper and no proper conditions derived from the physicochemical analysis.
3. To perform a kinetic study for proposing a growing mechanism of the ZnS deposited films.
4. To characterize the deposited samples in order to obtain the morphological, chemical, optical, and structural properties that allow inferring the best applications of the deposited ZnS films.

CHAPTER 1

ZINC SULFIDE PREPARED BY CHEMICAL BATH DEPOSITION

1.1. Chemical bath deposition technique

Chemical bath deposition (CBD) is a method that has been applied successfully in the production of thin film semiconductor materials. The technique was developed into the nineteenth century for the synthesis of thin films of lead sulfide and since then, it has been used to obtain other semiconductors with metals such as tin, manganese, cadmium and zinc, among others. It is a very attractive method due to the advantages that it offers over other deposition techniques: its simple implementation, non-sophisticated equipment required, relatively low temperatures below water boiling point for deposition, and large area deposition at low cost [1]. In the CBD technique, the growth process is carried out by a controlled chemical reaction in aqueous solution to deposit the desired material by precipitation [2].

1.1.1. Principles of the CBD technique

When a soluble salt, M_mX_n, is dissolved in water, a saturated solution is obtained in which the M^{n+} and X^{m-} ions are in contact with the residual of the non-dissolved M_mX_n solid. This situation originates an equilibrium condition between the dissolved ions and the solid phase in the solution according to the reaction:

$$M_m X_{n(s)} \leftrightarrow M^{n+}_{(aq)} + X^{m-}_{(aq)} \quad (1.1)$$

The relationship between the concentrations of the reactants and the products present in equilibrium of any chemical reaction can be expressed by the following equation:

$$K = \frac{[M^{n+}][X^{m-}]}{[M_m X_{n(s)}]} \quad (1.2)$$

where K is the equilibrium constant, $[M^{n+}]$, $[X^{m-}]$, and $[M_mX_{n(s)}]$ are the concentrations of the M^{n+} and X^{m-} ions, and the solid $M_mX_{n(s)}$, respectively. In the case of solids in aqueous solution its concentration is a constant number (K'= $[M_mX_{n(s)}]$). Since both the equilibrium constant and the concentration of the solid phase are constants, their product will also be constant. This value is called the solubility product (K_s) and the product $[M^{n+}][X^{m-}]$ is known as the ionic product, K_s [3]:

$$K_s = [M^{n+}][X^{m-}] \quad (1.3)$$

Precipitation will occur only when the ionic product exceeds the solubility product. In a CBD experiment, a substrate is immersed in an alkaline solution containing the chalcogenide ion (X^{m-}) and the metal source (M^{n+}), as can be seen in Figure 1. Chelating agents are added for controlling the concentration of the metal ions and releasing the chalcogenide ions. The particle size of the precipitates is determined by experimental conditions such as time, bath temperature, concentration of the chemical reagents, and agitation, among others.

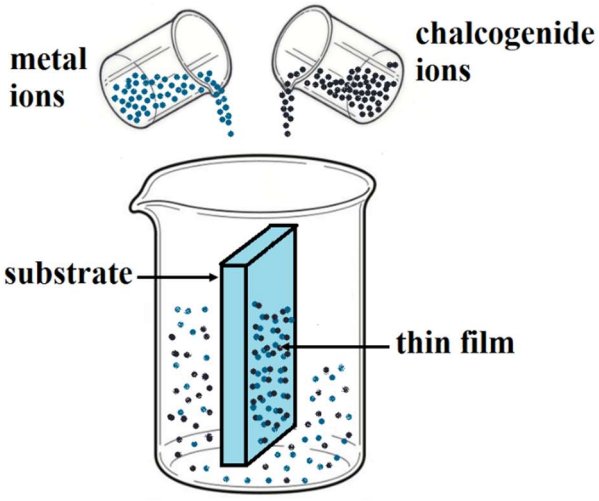

Figure 1.1. Representation of the deposition process of a thin film material by the CBD technique.

1.1.2. Metal chalcogenide films by the CBD technique

The compounds to be obtained by CBD must obey with this set of rules: the desirable compound can be obtained by simple precipitation; it should be highly insoluble in the used solution and should be chemically stable in the solution. The following compounds are some examples of materials obtained by CBD:

- *Lead sulfide (PbS)*

  Chemically deposited lead sulfide (PbS) thin films with its direct bandgap energy of 0.4 eV on glass substrates have satisfied the basic requirements for solar control coatings for window glazing applications in warm climates, where a low transmittance (10-30%) in the visible region is to be coupled with an appreciable reflectance for infrared radiation. In addition, PbS has been used as photoresistance, diode lasers, humidity and temperature sensors, decorative, and solar control coatings. These properties have been correlated with the growth conditions and the nature of substrates [4].

- *Cooper sulfide (Cu_xS)*

  It is a p-type semiconductor in which copper vacancies act as acceptors, indicating the strong dependence of electrical properties upon the deficit of copper atoms in Cu_xS. It can form five stable phases at room temperature: covellite CuS, anilite $Cu_{1.75}S$, digenite $Cu_{1.8}S$, djurleite $Cu_{1.95}S$, and chalcocite Cu_2S. It is potentially useful for different applications including solar control coatings, solar energy conversion, electronic and low temperature gas sensor applications [5].

- *Cadmium Selenide (CdSe)*

  CdSe has become quite interesting and important because of its major applications in solar cells due to its optimum bandgap energy (~1.75 eV), high absorption coefficient, and n-type of conductivity. With some additives, CdSe is attracting a great deal of attention owing to its potential and applied interests in a variety of thin film devices such as laser screen materials, projection color TVs, nuclear radiation detectors, and light emitting diodes [6].

- *Cadmium Sulfide (CdS)*

  Cadmium sulfide (CdS), due to its wide bandgap energy (2.42 eV), high photoconductivity, and high electron affinity, is known to be an excellent heterojunction partner for p-type cadmium telluride (CdTe), p-type copper indium diselenide ($CuInSe_2$), and/or $Cu(In,Ga)Se_2$ (CIGS). It has been widely used as an optical window material in high-efficiency thin film solar cells based on CdTe or CIGS. In 2011 a record of the efficiency of 20.1% was reached with a CdS/CIGS solar cell [7]. CdS has also been used in other applications including electronic and optoelectronic devices. The chemical mechanism of CdS prepared by CBD is

typically the thermal decomposition of thiourea ($CS(NH_2)_2$) in the presence of a cadmium salt in a basic aqueous solution containing ammonia (NH_3) [8].

1.2. Zinc Sulfide (ZnS)

Recently, the synthesis of ZnS by the CBD technique has been object of several studies, due to its use as an alternative semiconductor material to the CdS in thin film photovoltaic cells. The application of ZnS as a window layer allows a more effective photocurrent generation due to the larger bandgap energy of ZnS (3.72 eV) than that of CdS (2.40 eV) [9]. Using buffer layers of ZnS in solar cells, high efficiencies as 18.6% have been reported [10]. Actually, ZnS is an important semiconductor material. It has great potential to be used in thin film technology, such as optoelectronics (field-effect transistors, sensors) [11], electroluminescence devices (flat panel displays, light emitting diodes) [12] and photovoltaic technology (antireflection coating) [13]. ZnS has two structures, one with a cubic form called *zincblende* (ZnS-ZB) and another with a hexagonal structure named *wurtzite* (ZnS-WZ), as can be noted in Figure 1.2.

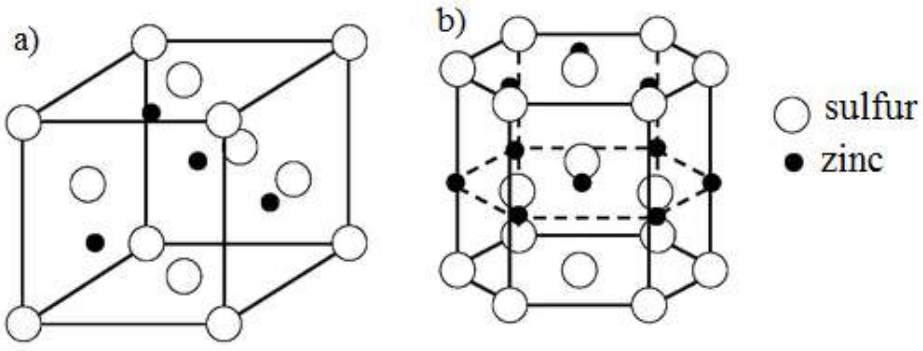

Figure 1.2. Crystalline structures for ZnS: a) zincblende, b) wurtzite.

The zincblende (ZB) structure consists of tetrahedral coordinate zinc and sulfur atoms packed in the ABCABC pattern, while the wurtzite (WZ) structure is stacked in the ABABAB pattern. The differences in the atomic arrangement lead to a large differences in properties [14]. ZnS-WZ has a bandgap energy (E_g) value of 3.77 eV, meanwhile for ZnS-ZB is 3.72 eV [15].

1.2.1. Applications of ZnS

Different applications of the ZnS have been reported in the literature, being the most important:

a) *Blue light emitting diode*: This application is due to the E_g value of 3.72 eV. The principle of operation is simple, a direct current is passed through the material before emitting light. To obtain the blue light emission is necessary to deposit a small layer of ZnS with high resistivity on another layer of ZnS with low resistivity in order to obtain a p-n junction and to obtain the diode effect [16].

b) *Anti-reflector*: It is used as a coating material on some materials for reducing glare. It is mainly used in the polycrystalline silicon solar cells [17].

c) *Optical window for solar cells of thin layer*: Its main function in this application is to pass the light coming from the Sun as a filter. By the high optical transmittance range in the ultraviolet and visible spectra, solar cells with efficiency of 18.6% have been reported [18].

1.2.2. Growing mechanism

For ZnS, a zinc salt solution can be converted into solid ZnS by mixing it in a solution containing sulfur ions. There are several routes for ZnS growth, but the following routes are the most reported:

1. Simple ionic reaction between zinc ions and sulfur ions (ion by ion) [19].

   The base of this mechanism is given by:

   $$Zn^{2+} + S^{2-} \rightarrow ZnS \tag{1.4}$$

   The growth mechanism involves the formation of sulfur ion (S^{2-}) and control of free zinc ion (Zn^{2+}). The process seems simpler, but it is more complicated since it comprises a high number of possible chemical reactions and equilibria.

2. Decomposition of a complex (L) [19]

   The following process involves several steps for the growth of ZnS:

   i) Complex ions diffusion and adsorption on the substrate.

   ii) Approximation of sulfide ions and relaxation of zinc/complex bond.

   iii) ZnS condensation on the surface and growth of the material

   Usually, this mechanism is summarized in the following reaction:

   $$(ZnL_n)^{2+} + S^{2-} \leftrightarrow ZnS + nL \tag{1.5}$$

3. Conversion of $Zn(OH)_2$ (hydroxide clusters) [21]

   A zinc hydroxide core is needed to allow growing the material. Then by means of an exchange reaction with the sulfur ions, the formation of the particles of ZnS is done, according to the following reaction:

   $$Zn(OH)_2 + S^{2-} \rightarrow ZnS + 2OH^- \tag{1.6}$$

1.2.3. Specific studies of ZnS deposition

In 1991, Lokhande [22] conducted a review on CBD-ZnS, and he provided a detailed and theoretical background of the CBD process. In the list of semiconductor materials that the author described, one of the pioneering works in the synthesis of ZnS by CBD was the one developed by Biswas *et al* [23]. This last group developed a method for the chemical deposition of ZnS thin films on a glass substrate at 55 °C and room temperature (30 °C) using Zn^{2+} salt solution, triethanolamine (TEA), sodium hydroxide, hydrazine hydrate, and thiourea as reacting agents. The prepared samples presented a ZnS-WZ crystalline structure and n-type in nature with bandgap energy of 3.68 eV. After this work, several investigations have been developed by different authors, bringing knowledge for improving and understanding the synthesis of ZnS by CBD. The following is a bibliographic revision of highlighted articles according to the specific topics of the deposition of ZnS by CBD.

1.2.3.1 Physicochemical studies

It is assumed that the chemical equilibrium among the species involved in the growth of ZnS by CBD is established rapidly, therefore the equilibrium models are useful for establishing the best conditions and for understanding the growth of the material. O'Brien and McAleesse [2] are pioneers in the use of these physicochemical models. The authors obtained the species diagram for zinc complexation and their comparison with the corresponding diagram for CdS at 55 °C (Figure 1.3).

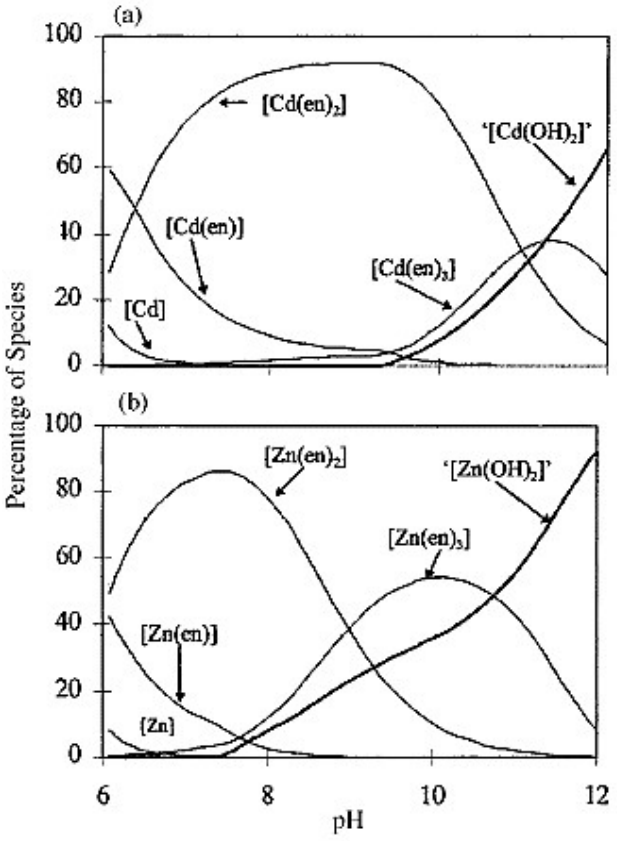

Figure 1.3. Species diagram for different complexes of (a) cadmium, and (b) zinc with hydroxide and ethylenediamine (en). Taken from reference [2]

They found notable differences in similar chemical baths for cadmium and zinc complexes. For example, in the alkaline region, the cadmium bath deposits CdS but the zinc bath provides zinc oxide (ZnO) or zinc hydroxide ($Zn(OH)_2$) more easily. They concluded that at high pH the system tends to lead the formation of $ZnO/Zn(OH)_2$, therefore it is necessary the presence of two complexants to enhance the decomposition of the sulfating agent, increasing the rate of growth of the film. Later, Hubert *et al.* [24] presented a thermodynamic study of the ZnS growing solution. Their purpose was to understand the effects of ammonia and the bath temperature on the deposition conditions and films composition. Their thermodynamic study was proposed by taking into account the pH of the

bath and the total concentrations of zinc and sulfide ions dissolved in solution and all the soluble complexes which can be formed in the system, but the hydrolysis of the thiourea was not taken into account. The solubility curves that they presented (Figure 1.4) showed that the addition of the ammonia involves the formation of ZnO and $Zn(OH)_2$ for a pH range between 7 and 12. By increasing the temperature, they observed a shift of the solubility region of all solid phases at lower pH.

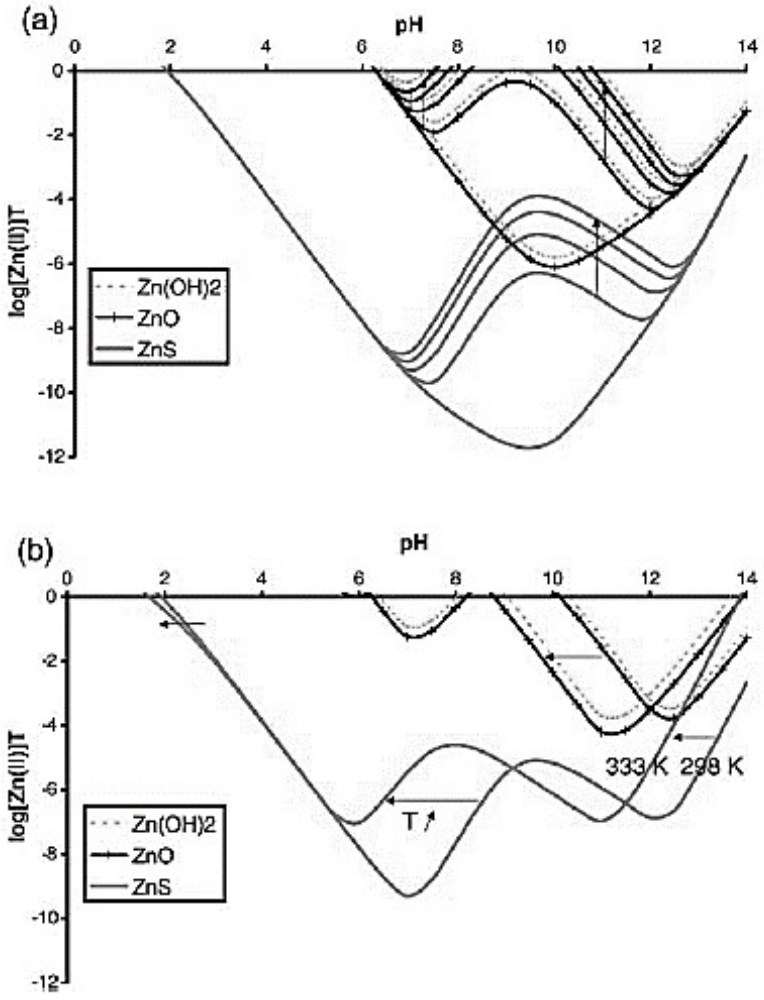

Figure 1.4 Effect of a) ammonia concentration, and b) temperature on the solubility of ZnS, ZnO and $Zn(OH)_2$. (Taken from reference [24]).

To confirm their calculations they synthesized ZnS at a bath temperature of 55 °C and they found that for lower concentrations of ammonia than 0.5 M, the $ZnO/Zn(OH)_2$ compounds precipitate immediately and for ammonia concentration up to 2 M, no deposition was observed.

In 2012, Tec-Yam *et al.* [25] developed a chemical analysis of the soluble species for predicting the optimal conditions to obtain high quality ZnS films. They identified the intermediate complexes in a species distribution diagram (SDD) that can be formed in a solution composed with zinc chloride ($ZnCl_2$), potassium hydroxide (KOH), ammonium nitrate (NH_4NO_3) and thiourea ($CS(NH_2)_2$) at 90 °C. The ZnS films exhibited high transmittance above 85 %, an E_g of 3.84 eV and a reflectance lower than 25 % in the UV-Vis range. Recently, González-Panzo *et al.* [26] established the best conditions to obtain ZnS films with high optical quality and good crystalline orientation. From an analytical model, they determined the SDDs and the solubility curves (SCs) from 50 to 90 °C (Figure 1.5).

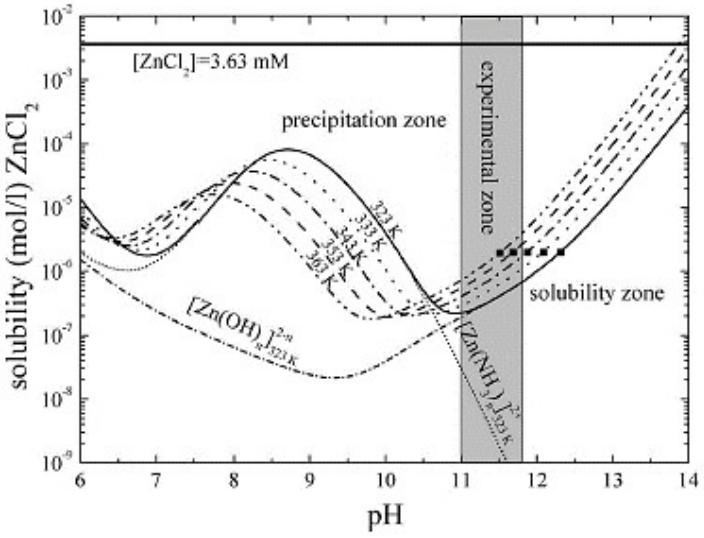

Figure 1.5 Solubility curves of $ZnCl_2$ at different temperatures as function of the solution pH (Taken from reference [26])

Each curve in Figure 1.5 represents the limit between the solubility and insolubility of the $ZnCl_2$ under different pH values and temperature conditions. Firstly, they demonstrated thermodynamically that precipitation is possible in a wide range of pH and temperature because of the concentration of $ZnCl_2$; that is, concentrations above of the plotted curves for each temperature. Secondly, they established the best conditions to obtain high quality ZnS films based on the SDD at 80 °C. These conditions coincide with the intersection in the SDDs plots of the $Zn(OH)_3^-$ and $Zn(OH)_4^{2-}$ species for a pH value of 11.7.

1.2.3.2 Kinetic studies

The aim of the kinetic studies is to obtain the best conditions for the deposition process and to explain the influence of the deposition time, concentrations of the chemical reagents and the bath temperature on the grown mechanism and quality of the films. One of the first investigations was carried out by Doña and Herrero [20] in 1994. They studied the effect of the bath temperature, for ZnS growth, in a range between 60 and 90 °C. They found that the growth of the material occurs in two stages, one of linear growth and one of saturation. They concluded that when the temperature increases, the growth rate also increases and calculated an activation energy (E_a) value of 20.9 kJ/mol. Later, Lui *et al.* [27] developed a kinetic study of their growth solution composed of zinc sulfate, thiourea and ammonia. They observed three different growth phases, a none-film one (induction), a quasi-linear one (growth) and a saturation one. In the quasi-linear region, film thickness can be controlled by deposition time control and from this region they calculated the initial growth rate. The variation of the growing rate (r) as a function of temperature (T) can be determined through the Arrhenius equation:

$$r(T) = Ae^{-\frac{E_a}{RT}} \tag{1.7}$$

where R is the molar gas constant and A is a constant related with the initial reagent concentration. The equation (1.7) can be plotted as the logarithm of the growth rate as a function of the inverse of the temperature between 60 and 90 °C (Figure 1.6).

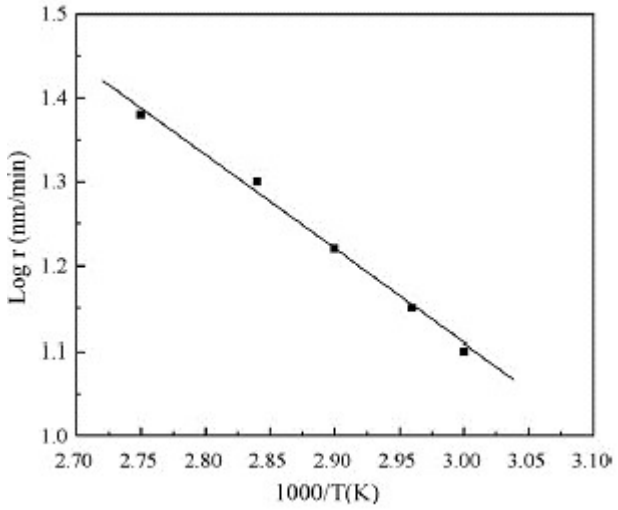

Figure 1.6. Linear adjustment of neperian logarithm of growth rate against the inverse of the temperature (Taken from reference [27]).

The slope of the linear adjustment of the data, gives the value of the activation energy which was estimated as 32.0 kJ/mol. By the low energy value obtained, they concluded that the rate of growth can be due by a physical process, such as diffusion or adsorption. Hubert *et al.* [28] studied experimentally the influence of the deposition parameters through the quartz crystal microgravimetry (QCM) technique. Figure 1.7 shows the measurements obtained through the QCM technique. By considering the effect of each reagent, authors observed that increase of zinc and thiourea and increase of pH up to 11.5 (Figs. 1.7 a, b, and d), respectively) leads to an increase of the growth rate; contrarily, an increase of ammonia concentration leads to an increase of the induction time and a decrease of the rate of growth

(Fig 1.7 e). Based on their results, this research group proposed the following equation for the rate of growth:

$$v = k\frac{[Zinc\ ^{0.7}[Thiourea\ ^{1.2}}{[Ammonia]^{0.4}[pH]^{1.0}} \quad (1.8)$$

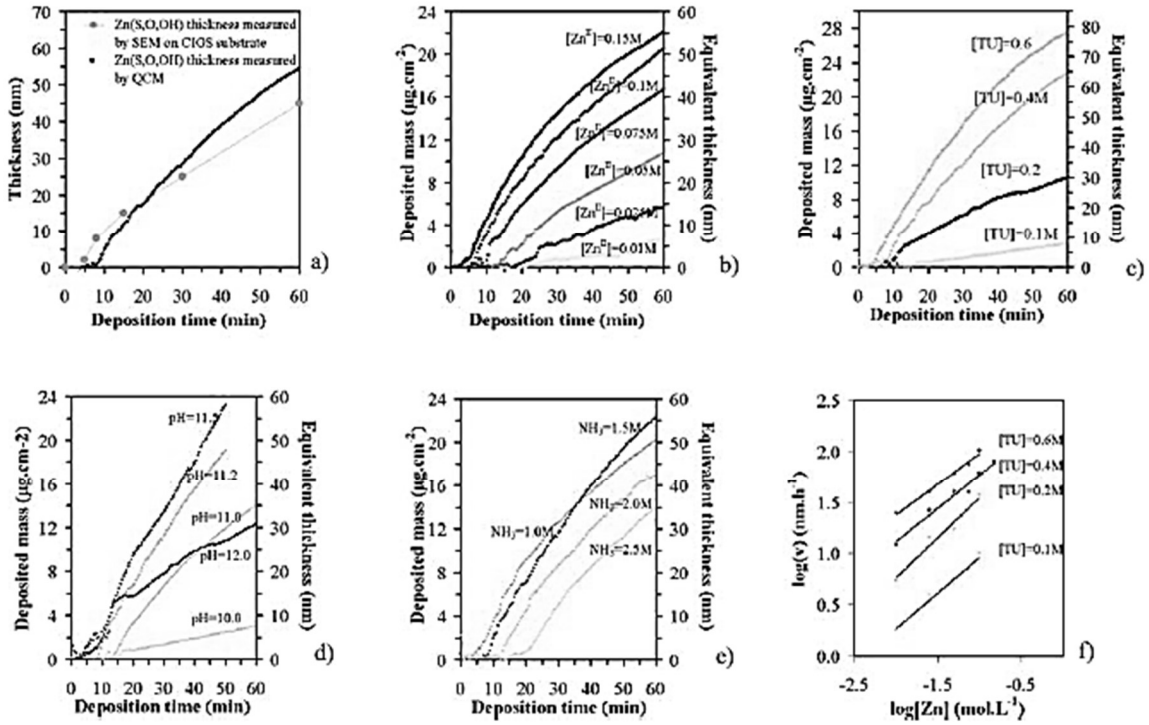

Figure 1.7. Measurements carried out by the QMC technique at different conditions (Taken from reference [28]).

The non-integer exponents and the value of 14.1 kcal mol^{-1} of the activation energy indicated that the process is controlled by chemical reactions at the surface of absorbers. Recently, Vallejo *et al.* [29], and González-Panzo *et al*. [30] reported activation energy calculations in their investigations for bath temperatures in the range from 60 to 90 °C, obtaining values of 33.6 and 44.9 kJ/mol respectively. In their experiment, Vallejo *et al.,* used a solution composed of zinc acetate, ammonia, sodium citrate and thiourea; meanwhile, González-Panzo *et al.*, used zinc chloride, potassium hydroxide, ammonium nitrate and

thiourea. Note that the evolution of the chemical reaction during the deposition process is strongly dependent on several parameters such as the type of chemical reagents, their concentrations, and the temperature of the chemical bath.

1.3. Goals of the work

As can be seen, there are many important contributions that are useful to understand and clarify the methodology of obtaining good quality ZnS thin films by CBD in a controlled way. As can be noticed, most of the studies on ZnS deposited by CBD report chemical reactions taking place at temperatures above 60 °C. Scarce literature regarding analysis and procedures for depositing ZnS films at near room conditions (below 50 °C) can be found, and the resulting properties of the films grown under these conditions are still unexplored. The ZnS growth at temperatures close to room conditions becomes an issue of interest for the technological industry due to the potential of scalability, as the fabrication process can be easily implemented and reduction of energy use for the growth process could be possible.

In this thesis, the growth and characterization of ZnS films deposited onto glass substrates by the CBD technique at bath temperatures of 25, 32, 40, 47 and 55 °C (near room conditions) are investigated. Species distributions diagrams and solubility curves were elaborated at different conditions in order to obtain the best conditions for synthesizing high quality ZnS thin films. The effect of the chemical bath temperature on the dynamic evolution of the ZnS growth is also investigated. In addition, chemical, morphological, optical and structural properties of deposited ZnS films obtained at different temperatures and chemical conditions are discussed.

CHAPTER 2

PHYSICOCHEMICAL ANALYSIS

As mentioned in the previous Chapter, for depositing a compound by the CBD technique, its ionic product must exceed its solubility product. In the case of ZnS films, this requirement occurs by the following condition [31]:

$$[Zn^{2+}][S^{2-}] \geq K_{ps} \tag{2.1}$$

However, the fulfillment of this condition depends on the species present in the solution and on the chemical reagents used for growing the semiconductor material. Thus, it is necessary to develop a physicochemical model that allows analyzing the concentrations of each species presents in the solution for determining the dominant ions present in the active chemical species in solution.

2.1. Speciation model

In this work, zinc chloride ($ZnCl_2$) is used as the source of zinc ions (Zn^{2+}), ammonium nitrate (NH_4NO_3) and potassium hydroxide (KOH) as pH regulators and complexing agents, and thiourea ($SC(NH_2)_2$) as the source of sulfur ions (S^{2-}). From the combination of these reagents, different zinc complexes and thiourea derivatives can be obtained as well as free ions such as Zn^{2+}, ammonia (NH_3), hydroxide (OH^-) and hydronium (H^+). The main chemical reactions that take place in the aqueous solution once the reagents are mixed. On the left side, the most probable chemical reactions are shown, while on the right side the calculations of the equilibrium constant (K) are enlisted for each corresponding chemical reaction.

a) Decomposition of thiourea and dissociation of hydrogen sulfide

$$SC(NH_2)_{2(aq)} \leftrightarrow H_2S_{(aq)} + H_2NCN_{(aq)} \qquad K_1 = \frac{[H_2S][H_2NCN]}{[SC(NH_2)_2]} \tag{2.2}$$

$$H_2S_{(aq)} \leftrightarrow HS^-_{(aq)} + H^+_{(aq)} \qquad K_2 = \frac{[HS^-][H^+]}{[H_2S]} \tag{2.3}$$

$$HS^-_{(aq)} \leftrightarrow S^{2-}_{(aq)} + H^+_{(aq)} \qquad K_3 = \frac{[S^{2-}][H^+]}{[HS^-]} \tag{2.4}$$

$$H_2NCN_{(aq)} \leftrightarrow HNCN^-_{(aq)} + H^+_{(aq)} \qquad K_4 = \frac{[HNCN^-][H^+]}{[H_2NCN]} \tag{2.5}$$

$$HNCN^-_{(aq)} \leftrightarrow NCN^{2-}_{(aq)} + H^+_{(aq)} \qquad K_5 = \frac{[NCN^{2-}][H^+]}{[HNCN^-]} \tag{2.6}$$

b) Dissociation of water and formation of hydroxi-complexes.

$$H_2O_{(l)} \leftrightarrow H^+_{(aq)} + OH^-_{(aq)} \qquad K_6 = \frac{[H^+][OH^-]}{[H_2O]} \tag{2.7}$$

$$Zn^{2+}_{(aq)} + OH^-_{(aq)} \rightarrow Zn(OH)^+_{(aq)} \qquad K_7 = \frac{[Zn(OH)^+]}{[Zn^{2+}][OH^-]} \tag{2.8}$$

$$Zn^{2+}_{(aq)} + 2OH^-_{(aq)} \rightarrow Zn(OH)_{2(aq)} \qquad K_8 = \frac{[Zn(OH)_2]}{[Zn^{2+}][OH^-]^2} \tag{2.9}$$

$$Zn^{2+}_{(aq)} + 3OH^-_{(aq)} \rightarrow Zn(OH)^-_{3(aq)} \qquad K_9 = \frac{[Zn(OH)^-_3]}{[Zn^{2+}][OH^-]^3} \tag{2.10}$$

$$Zn^{2+}_{(aq)} + 4OH^-_{(aq)} \rightarrow Zn(OH)^{2-}_{4(aq)} \qquad K_{10} = \frac{[Zn(OH)^{2-}_4]}{[Zn^{2+}][OH^-]^4} \tag{2.11}$$

c) Dissociation of ammonium and formation of amino-complexes

$$NH^+_{4(aq)} \rightarrow NH_{3(aq)} + H^+_{(aq)} \qquad K_{11} = \frac{[NH_3][H^+]}{[NH^+_4]} \tag{2.12}$$

$$Zn^{2+}_{(aq)} + NH_{3(aq)} \rightarrow Zn(NH_3)^{2+}_{(aq)} \qquad K_{12} = \frac{[Zn(NH_3)^{2+}]}{[Zn^{2+}][NH_3]} \tag{2.13}$$

$$Zn^{2+}_{(aq)} + 2NH_{3(aq)} \rightarrow Zn(NH_3)^{2+}_{2(aq)} \qquad K_{12} = \frac{[Zn(NH_3)^{2+}_2]}{[Zn^{2+}][NH_3]^2} \qquad (2.14)$$

$$Zn^{2+}_{(aq)} + 3NH_{3(aq)} \rightarrow Zn(NH_3)^{2+}_{3(aq)} \qquad K_{12} = \frac{[Zn(NH_3)^{2+}_3]}{[Zn^{2+}][NH_3]^3} \qquad (2.15)$$

$$Zn^{2+}_{(aq)} + 4NH_{3(aq)} \rightarrow Zn(NH_3)^{2+}_{4(aq)} \qquad K_{15} = \frac{[Zn(NH_3)^{2+}_4]}{[Zn^{2+}][NH_3]^4} \qquad (2.16)$$

d) Formation of precipitates

$$ZnS_{(s)} \rightarrow Zn^{2+}_{(aq)} + S^{2-}_{(aq)} \qquad K_{psZnS} = [Zn^{2+}][S^{2-}] \qquad (2.17)$$

$$Zn(OH)_{2(s)} \rightarrow Zn^{2+}_{(aq)} + 2OH^{-}_{(aq)} \qquad K_{psZn(OH)_2} = [Zn^{2+}][OH^{-}]^2 \qquad (2.18)$$

In a previous effort, reported by González-Panzo *et al.,* [26], a physicochemical model was developed. The authors show the dependence of the bath temperature and the importance of simultaneously considering all the reactions mentioned above. They calculated the equilibrium constants of all the presented reactions through the change of enthalpy of the system by performing a linear adjustment to the values of the equilibrium constants previously reported, according to the following equation:

$$\log K = A + \frac{B}{T} + C \cdot logT \qquad (2.19)$$

where A, B and C are constant values in each chemical reaction. They also took into account the mass balance of thiourea, ammonium, and zinc, as well as the charge balances. An analytical model was determined for calculating the concentrations of all the formed species in the chemical solution according to:

a) From the pH value (as rough approximation), the concentration of H^+ ions was estimated for obtaining the concentration value of S^{2-} ions.

b) In the saturation line, the concentration of the Zn^{2+} ions is defined by at least one of the solubility equilibria (Eqs. 2.17 and 2.18), by using the S^{2-} and OH^- values for calculation.

c) The free ammonium concentration with the obtained concentrations of Zn^{2+} and OH^- is also estimated.

This physicochemical model was developed for a range of temperature between 60 and 90 °C, so it is necessary to make an adjustment to the equilibrium constants to be used at temperatures below 60 °C. The values of the equilibrium constants were generated with Eq. (2.19) by taking the values of the constants *A*, *B* and *C* reported in the work of Isidro *et al.* [26]. Table 2.1 shows these calculated values for the five temperatures used in this work: 25 °C (298 K), 32 °C (305 K), 40 °C (313 K), 47 °C (320 K), and 55 °C (328 K). In order to determine the best conditions for the growth of ZnS, the solubility curves (SCs) and the species distribution diagrams (SDDs) were generated for these temperatures. SCs and SDDs are obtained with the concentrations of each species and the equilibrium constants of all the reactions (listed in Table 2.1) at a desired temperature. The SCs and SDDs are plotted as a function of pH considering the equilibrium expressions of each species in the solution. It is important to note that in the thermodynamic condition, Eq. (2.1), the concentrations of sulfur and zinc ions play a very important role; therefore, it is necessary to establish proper parameters such that the ZnS material can be deposited.

A Matlab program that integrates all the chemical reactions and conditions proposed in Table 2.1 is used to find the concentration of each species in the solution (See Figure 2.1). The program has as input data the concentration of each of the chemical reagents and the deposition temperature, and as output data, the produced species concentrations, and the

solubility as a function of the pH of the solution. In this work, both SCs and SDDs were generated for the Zn-NH_3-OH-$SC(NH_2)_2$ system and the pH of the solution for the five proposed temperatures. The thiourea concentration was varied in order to establish the most suitable pH region for depositing the high quality ZnS thin films, meanwhile the concentration of the other reagents remained constant.

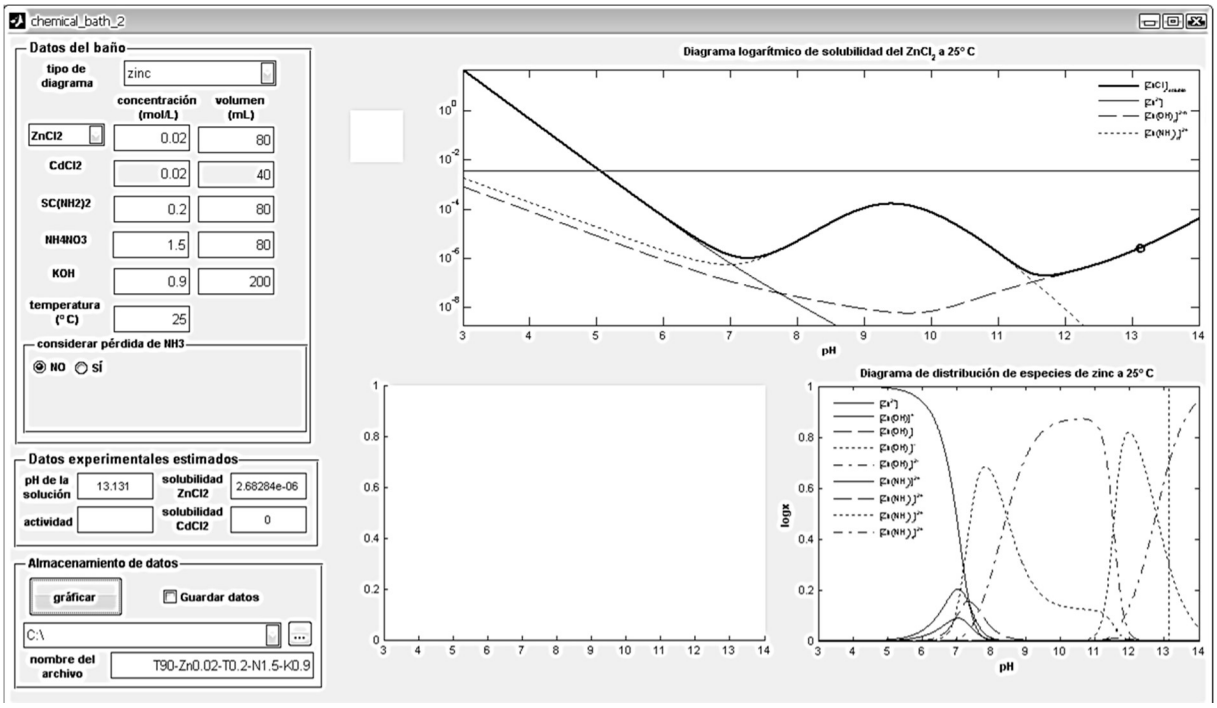

Figure 2.1. Matlab program homepage used to obtain the SCs and SDDs.

2.2. Physicochemical analysis at room temperature (25 °C)

Since the solubility product of ZnS is low (log K = -29.305), precipitation of the ZnS can takes place at low concentrations of the Zn^{2+} and S^{2-} ions. If the Zn^{2+} ions concentration is established as an initial parameter, the thermodynamic condition, Eq. (2.1), is a function of the concentration of S^{2-} ions; therefore, it is necessary to adjust its concentration to fulfill this condition.

Table 2.1 Values of the equilibrium constant of the different reactions at different temperatures.

Chemical reaction	Log K				
	298 K	305 K	313 K	320 K	328 K
$SC(NH_2)_2 \leftrightarrow H_2S + H_2NCN$	-23.430	-21.962	-21.515	-21.121	-20.669
$H_2S \leftrightarrow HS^- + H^+$	-7.338	-6.892	-6.798	-6.727	-6.658
$HS^- \leftrightarrow S^{2-} + H^+$	-17.742	-17.087	-16.920	-16.783	-16.636
$H_2NCN \leftrightarrow HNCN^- + H^+$	-10.668	-10.254	-10.141	-10.046	-9.941
$HNCN^- \leftrightarrow NCN^{2-} + H^+$	-12.105	-10.966	-10.696	-10.481	-10.258
$H_2O \leftrightarrow H^+ + OH^-$	-14.753	-13.772	-13.532	-13.338	-13.133
$Zn^{2+} + OH^- \rightarrow Zn(OH)^+$	6.199	6.297	6.348	6.400	6.467
$Zn^{2+} + 2OH^- \rightarrow Zn(OH)_2$	10.030	10.051	10.086	10.148	10.223
$Zn^{2+} + 3OH^- \rightarrow Zn(OH)_3^-$	13.652	13.800	13.956	14.168	14.386
$Zn^{2+} + 4OH^- \rightarrow Zn(OH)_4^{2-}$	14.675	14.871	15.073	15.343	15.615
$NH_4^+ \rightarrow NH_3 + H^+$	-9.908	-9.039	-8.811	-8.621	-8.413
$Zn^{2+} + NH_3 \rightarrow Zn(NH_3)^{2+}$	2.595	2.388	2.344	2.311	2.279
$Zn^{2+} + 2NH_3 \rightarrow Zn(NH_3)_2^{2+}$	5.226	4.825	4.718	4.629	4.531
$Zn^{2+} + 3NH_3 \rightarrow Zn(NH_3)_3^{2+}$	8.801	7.552	7.264	7.038	6.807
$Zn^{2+} + 4NH_3 \rightarrow Zn(NH_3)_4^{2+}$	9.954	9.026	8.758	8.526	8.264
$ZnS_{(s)} \rightarrow Zn^{2+} + S^{2-}$	-29.305	-28.210	-27.943	-27.729	-27.504
$Zn(OH)_{2(S)} \rightarrow Zn^{2+} + 2OH^-$	-17.351	-16.767	-16.650	-16.566	-16.489

However, given the equilibrium constants values obtained from the thiourea dissociation sequence, Eqs. (2.3), (2.4), and column 298 K in Table 2.1, it can be noted that bisulfide ions (HS^-) will be the species with highest presence in the solution (small values of equilibrium constants favor its formation), and therefore they will be responsible for contributing to the growth of the material. On the other hand, there are several species of zinc (Zn^{2+}, amino- and hydroxy-complexes) that can take part in the solution for ZnS deposition. The formation of each complex depends largely on the pH of the growth solution.

In order to determine the ideal pH that fulfill with the thermodynamic condition, the SCs of the different species as a function of the thiourea concentration (Fig. 2.1) were obtained. The labels in Fig. 2.1 have the following significance: the line L-Zn^{2+} represents the concentration of the Zn^{2+} ions; the L-$Zn(NH_3)$ denotes the total concentration of all amino-complexes ($Zn(NH_3)^{2+}$, $Zn(NH_3)_2^{2+}$, $Zn(NH_3)_3^{2+}$, $Zn(NH_3)_4^{2+}$) ions, while the line L-Zn(OH) indicates the total concentration of all the species of hydroxy-complexes ($Zn(OH)^+$, $Zn(OH)_2$, $Zn(OH)_3^-$, $Zn(OH)_4^{2-}$) ions. Finally, the L-S line means the total concentration of the sulfur species (H_2S, HS^-, S^{2-}).

It can be observed from Fig. 2.2 the existence of three zones where the zinc species do not change when the concentration of thiourea is varied. The first one (free zinc zone), where the Zn^{2+} ion dominate, is located at pH < 7. In the second zone (amino zone), the amino-complexes have greater presence when the pH ranges from 7 to 11.5, meanwhile the hydroxy-complexes dominate in the solution with pH > 11.5 (hydroxide zone). On the other hand, the L-S lines present a similar behavior for all the concentrations of thiourea.

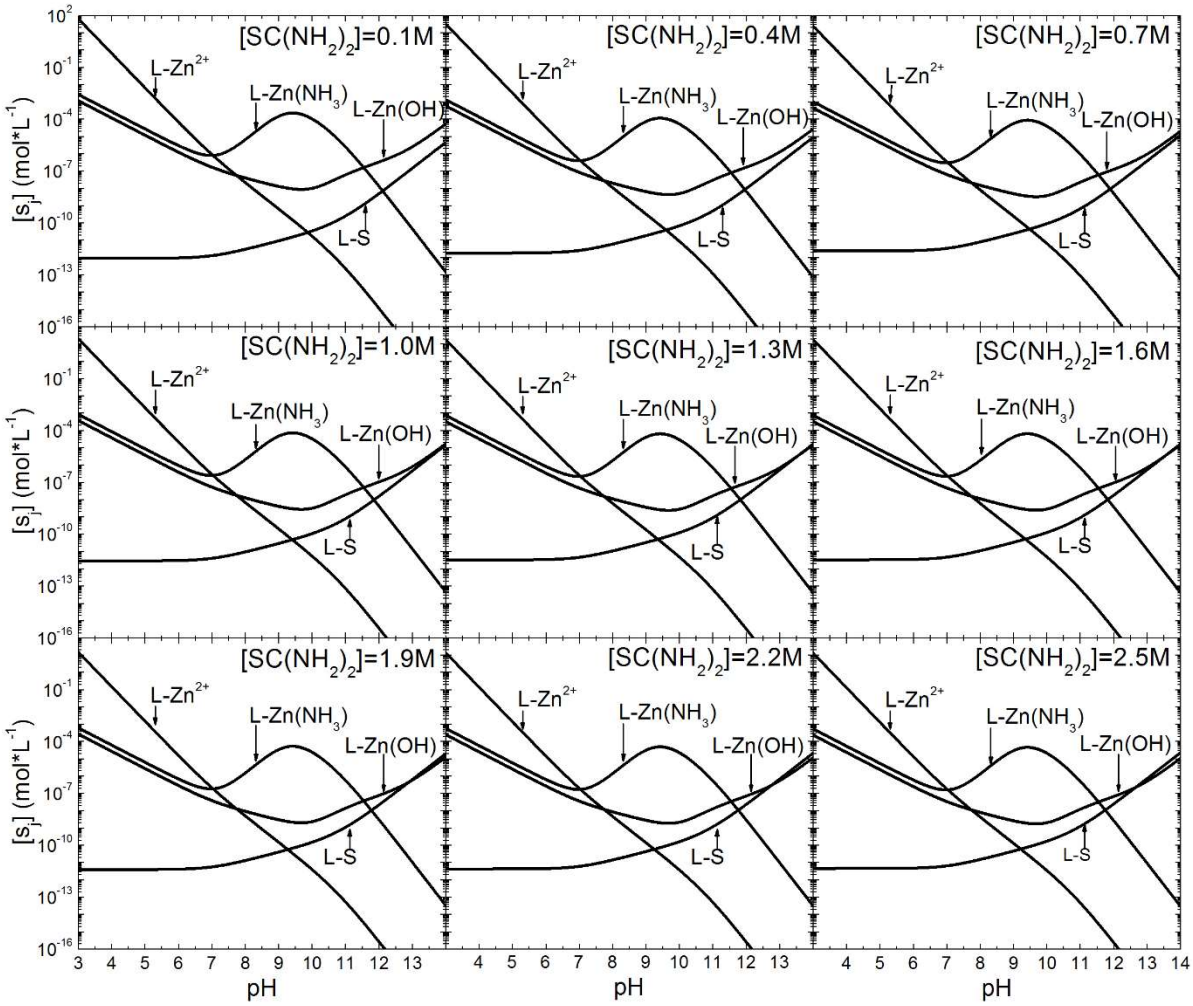

Figure 2.2 Solubility curves obtained at 25 °C for different thiourea concentrations.

This last line remains constant across the free zinc region, increases slightly in the amino zone and shows an even bigger increase on the hydroxide region. In this behavior, the thiourea needs OH^- ions to dissociate and release sulfur ions in the solution [20]. According to the growth mechanisms of ZnS discussed in Section 1.2.2 and their corresponding SCs, it can be noted that the ion-ion mechanism is more likely to occur in the free zinc zone, when the pH value is below 7. The decomposition of a complex mechanism could be carried out in the area where the amino-complexes dominate, in the range of pH between 7 and 11.5. Finally, the growth mechanism by hydroxides would take place in the area where pH is higher

than 11.5. These three growth mechanisms depend strongly on the concentration of sulfur ions in the solution. If this quantity is very small, the value of the solubility product cannot be exceeded; therefore, the ZnS will not be formed (*thermodynamic condition*). On the other hand, from Eq. (2.17), one S^{2-} ion is required for each Zn^{2+} ion so that the ZnS growth process can be carried out optimally (*stoichiometric condition*).

In Figure 2.2, for 0.1 M as thiourea concentration, in the free zinc zone, the concentration of the sulfur species is very small as compared to the Zn^{2+} ion (the solubility lines are separated by several orders of magnitude) and although the ionic product exceeds the solubility product of the material, difficult ZnS growth is given the excess of zinc in the solution. As the concentration of thiourea increases, the L-S line shows a slight increase while the L-Zn^{2+} line decreases, but the difference between them remains quite large, and the ZnS growth conditions are not optimal. Therefore, in this zone the thermodynamic condition is satisfied, but not the stoichiometric. In a similar way, this behavior occurs in the amino zone for all the thiourea concentrations studied, where, in spite of a greater increase in the concentration of sulfur species, the L-S line remains below the L-Zn(NH_3) line. Therefore, the growth processes described in Eqs. (1.4) and (1.5), although they satisfy the *thermodynamic condition* of the solubility product, are unlikely to occur because there is not enough sulfur species in the solution at these pH zones and the *stoichiometric condition* is not satisfied. In the hydroxide zone there is a high concentration of the sulfur species as compared to the other two zones and, as mentioned before, thiourea needs OH^- ions to decompose and release different sulfur species causing the complexation of zinc and hydroxides decreasing. This condition produces a major separation between the hydroxy-complexes and the sulfur species lines decreases considerably, reaching a point where the L-S line completely exceeds the L-Zn(OH) line as can be noted in Figure 2.3. This fact can be

observed for the first time when the thiourea concentration is 1.3 M. The lines of sulfur and hydroxy-complexes intersect in pH = 13.55 (dashed line in the inset of Fig. 2.3), and in this value (named *solubility cross-point*) the L-S line exceeds that of the hydroxides.

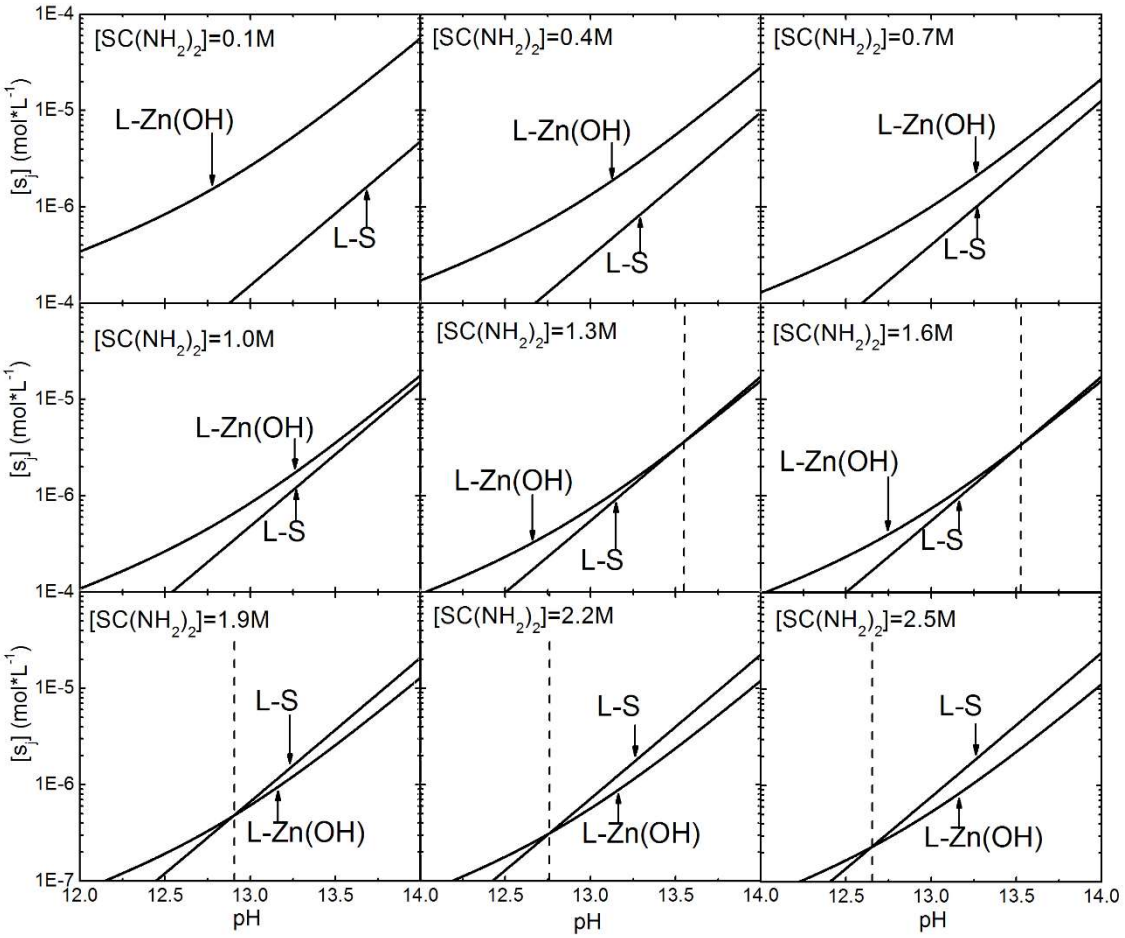

Figure 2.3. Zoomed-view of the SCs where the L-S and L-Zn(OH) cross-point is shown.

Lower pH values produce solutions rich in zinc species, while higher pH values, poorer solutions. In the *solubility cross-point* equality is established between the concentration of the sulfur species and the hydroxy-complexes, such that the *stoichiometric condition* is satisfied. By increasing the concentration of thiourea, the *solubility cross-point* takes place at lower pH values. For example, when the thiourea concentrations are 1.90 M,

2.20 M, and 2.50 M, the *solubility cross-point* is found at pH values of 12.90, 12.80, and 12.65, respectively. In order to establish the parameters for satisfying the *stoichiometric condition* it is necessary to know which type of species are actively involved in the growth of ZnS.

Species distribution diagrams (SDDs) are used to identify the mainly active ions in the solution. SDDs give the molar fraction (r_i) of each species as a function of the pH of the solution. The value of r_i is obtained by dividing the molar concentration of a certain species and the sum of all the species involved, that is:

$$r_i = \frac{[s_i]}{\sum_i [s_i]} \tag{2.20}$$

Figure 2.4 shows the SDDs for the conditions given in Figure 2.2, at 25 °C, and variations in thiourea form 0.1 to 2.5 M. The considered species are all those with active participation in the deposition of the ZnS, that is, the Zn^{2+} ion, the eight zinc complexes species ($Zn(NH_3)^{2+}$, $Zn(NH_3)_2^{2+}$, $Zn(NH_3)_3^{2+}$, $Zn(NH_3)_4^{2+}$, $Zn(OH)^{+}$, $Zn(OH)_2^{0}$, $Zn(OH)_3^{-}$, $Zn(OH)_4^{2-}$) and the three species of sulfur (H_2S, HS^-, S^{2-}). From the solubility curves, the zone below pH=10.50 must be disregarded because the probability of ZnS formation is negligible, such that only the pH-range above 10.50 was considered.

As mentioned, from Figure 2.2, the bisulfide ion is the predominant species of all the sulfur species, given its largest molar fraction. The presence of the HS^- ions begin for pH = 11 and increases with the increased pH value. From the zinc species, all the hydroxy-, tri- and tetra-hydroxide complexes present the greatest participation in the solution, the first one in the $11.50 < pH < 12.77$ range, and the second one for $pH > 12.77$. Unlike the mechanism proposed in Eq. (1.6), zinc hydroxide is not the major species in the hydroxide zone; whereby, such deposition mechanism could not be carried out as is proposed. The most suitable

conditions to obtain ZnS at 25 °C involve three main ions: $Zn(OH)_3^-$, $Zn(OH)_4^{2-}$, and HS^-. The tri- and tetra- hydroxy complexes would be mediators for the formation of the ZnS nuclei which react subsequently with the HS^- ion through an ionic exchange reaction.

$Zn(OH)_2$ has a solubility product larger than ZnS, which allows the sulfur ions to completely replace the OH^- ions in the growing process, but the difference between these values may cause that the ionic exchange cannot be carried out completely [32]. Thus, it is important to have enough sulfur species to improve the probability for obtaining only ZnS throughout the growth process. The characteristics and particularities of the growth mechanism will be discussed in depth in the subsequent chapters. In summary, the mechanism for growing ZnS at room temperature can be described by the following equations:

$$Zn(OH)_3^- + HS^- \rightarrow ZnS + OH^- + H_2O \quad (2.21)$$

$$Zn(OH)_4^{2-} + HS^- \rightarrow ZnS + OH^- + 2H_2O \quad (2.22)$$

For each mole of hydroxide complex one mole of HS^- is required for obtaining ZnS with ideal stoichiometry. Therefore, it can be inferred that equal concentrations of $Zn(OH)_3^-$ and $Zn(OH)_4^{2-}$ ions are required and the following chemical reaction needs to be satisfied:

$$\frac{[HS^-]}{[Zn(OH)_4^{2-}]} = \frac{[HS^-]}{[Zn(OH)_3^-]} = 2 \quad (2.23)$$

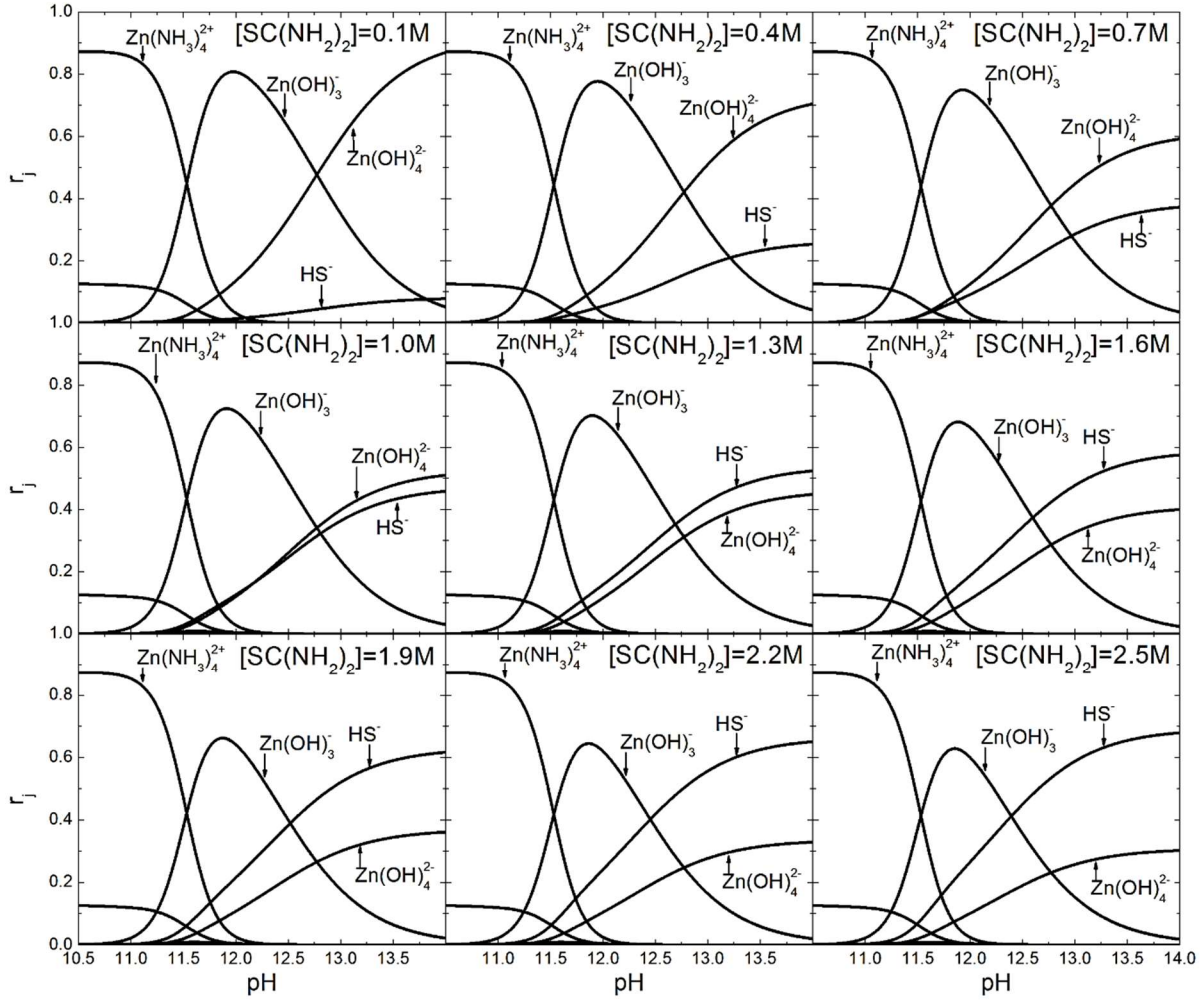

Figure 2.4 Species distribution diagrams (SDDs) for ZnS formation under different thiourea concentrations at 25°C.

Eq. (2.23) is the *stoichiometric condition* that must be fulfilled to obtain adequate formation of the ZnS by the CBD technique. From Figure 2.4, the pH value in which the $Zn(OH)_3^-$ and $Zn(OH)_4^{2-}$ ions present the same concentration, is the intersection of the molar fraction lines (called *hydroxide cross-point*) which occurs at pH = 12.77. An increase of the thiourea concentration does not modify the *hydroxide cross-point* and only the value of its molar fraction is modified. When the thiourea concentration is below 1.3 M, the molar fraction of the HS^- ions is under the value of the molar fraction of the *hydroxide cross-point*,

and the stoichiometry condition would not be fulfilled, which lead to a stoichiometric imbalance. Therefore, it is not convenient to synthesize the ZnS with concentrations of thiourea below 1.3 M. When the concentration of thiourea is 1.3 M, at the *hydroxide cross-point*, the molar fraction of the HS^- ions exceed that of the $Zn(OH)_3^-$ and $Zn(OH)_4^{2-}$ ions, but Eq. (2.23) is not satisfied. For the *solubility cross-point* at this concentration, the sum of the concentrations of the hydroxy-complexes is equal to the concentration of the HS^- ions; however, the stoichiometry will not be correct, due to higher concentration of $Zn(OH)_4^{2-}$ ions in comparison with the $Zn(OH)_3^-$ ions. For the cross-point (*hydroxide* and *solubility*) with known pH value, described Eq. (2.23) is achieved and the thermodynamic and stoichiometry conditions are fulfilled, producing an optimal growing of ZnS. Taking into account the solubility cross-points of the other thiourea concentrations, the value of 2.2 M has the greatest similarity between the *solubility cross-point* and the *hydroxides cross-point*. With this concentration of thiourea there is a slight variation of 0.03 between the cross-points, and the ratio described in Eq. (2.23) would be of 1.96. Making a final adjustment to the concentration of thiourea to obtain the value in which the growth of the material can be optimally obtained, it is estimated that with a thiourea concentration of 2.25 M, the *solubility cross-point* coincides with the *hydroxide cross-point,* as shown in Figure 2.5, ensuring confidence with the thermodynamic and stoichiometric conditions required for optimum ZnS growth.

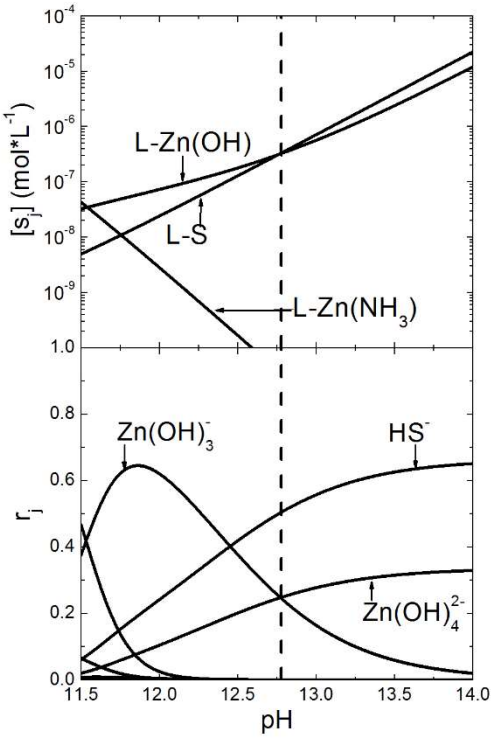

Figure 2.5. SC and SDD plots obtained with thiourea concentration of 2.25 M for obtaining optimal deposition of ZnS.

2.3. Physicochemical analysis for temperatures close to the ambient

Following a similar physicochemical analysis performed for the other deposition temperatures (32, 40, 47, and 55 °C), the thiourea concentrations values to ensure proper conditions for ZnS growth are estimated as: 0.70 M for 55 °C, 0.95 M for 47 °C, 1.25 M for 40 °C, and 1.70 M for 32 °C. The first effects of temperature can be observed in the equilibrium constants listed in Table 2.1. For species containing sulfur, an increment in the equilibrium constant value results in a greater dissociation of thiourea, and therefore, in an increment in concentration of the different sulfur ions. For zinc species, there is also a change in concentration, as can be observed in the solubility curves in Figure 2.6 for temperatures of 32 and 55°C with thiourea concentrations of 0.7 and 1.7 M, respectively.

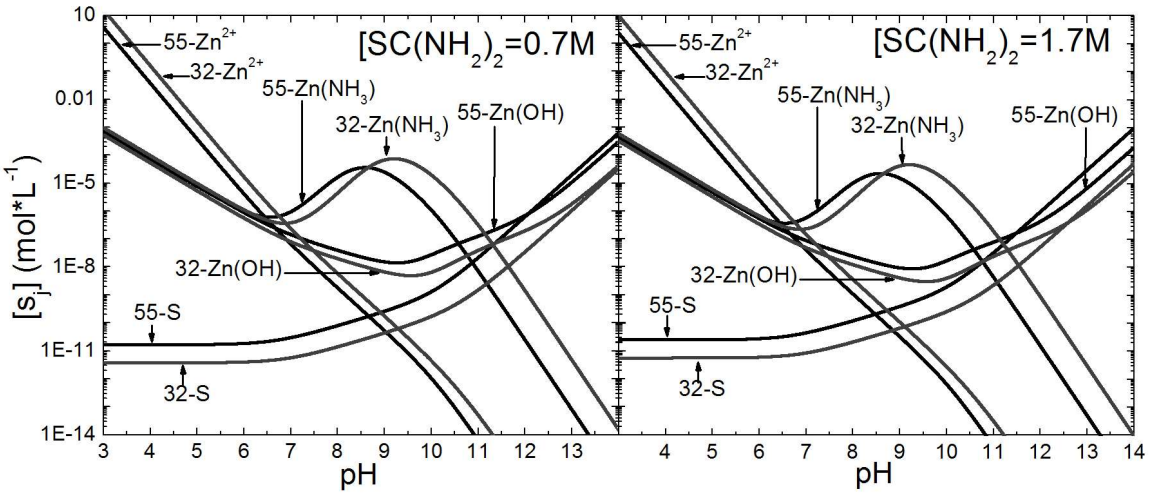

Figure 2.6. Solubility curves for two different thiourea concentrations at 32 °C and 55 °C.

The behavior of the zinc ions varies depending on the nature of them. For the same concentration of thiourea, there is a decrease in the concentration of the Zn^{2+} ions and the amino-complexes, but in contrast, there is an increase in the amount of hydroxy-complexes available in the solution. This situation is because when the temperature increases, the equilibrium constants of the amino-complexes decrease causing a smaller number of them, while the constants of the hydroxy-complexes rise, increasing their concentration. As for the *solubility cross-point*, note that there is a shift towards lower values of the pH when the temperature increases, as shown in Table 2.2, because of the increase of the equilibrium constant value of the water. Hence, the optimal pH value for growing ZnS films shifts to lower values with increasing temperature and with changes in the solubility curves. This effect is beneficial to the growth process, since $Zn(OH)_2$ formation can be avoided without impairing optimum growth conditions.

Table 2.2. *pH values of the solubility cross-points for different temperatures and thiourea concentrations.*

$[SC(NH_2)_2]$ (M)	Bath temperature (°C)			
	32	40	47	55
0.70	- - -	13.40	12.59	12.10
0.95	13.60	12.71	12.25	11.85
1.25	12.95	12.42	12.03	11.66
1.70	12.60	12.17	11.85	11.47

The particular effect of the temperature on the different ions in solution can be observed in Figure 2.7. The labels on each graph indicate the temperature and concentration of the thiourea on which the analysis was performed. For example, 32-T0.7M means that the deposition was carried out at 32 °C with a thiourea concentration of 0.7 M. Analyzing in a particular way the behavior of each species it can be noted a shift of the species towards lower pH values with the increase of temperature. For example, when the thiourea concentration is of 0.7 M, the *hydroxide cross-point* at 32°C is at pH = 12.66, while at 55°C the pH = 12.10.

As mentioned above, an increasing in temperature, promotes the decomposition of thiourea [33] since thermal energy is supplied to the solution which facilitates the hydrolysis of the thiourea and leads to an increase of the molar fraction of the HS^- ions, producing a decrease of the hydroxy-complexes by consuming the OH^- ions in the solution. In conclusion, Table 2.3 shows the optimal conditions (thiourea concentrations and pH values of the solution) for synthesizing the ZnS material at near ambient temperatures, where the thermodynamic and stoichiometric conditions of the system are satisfied.

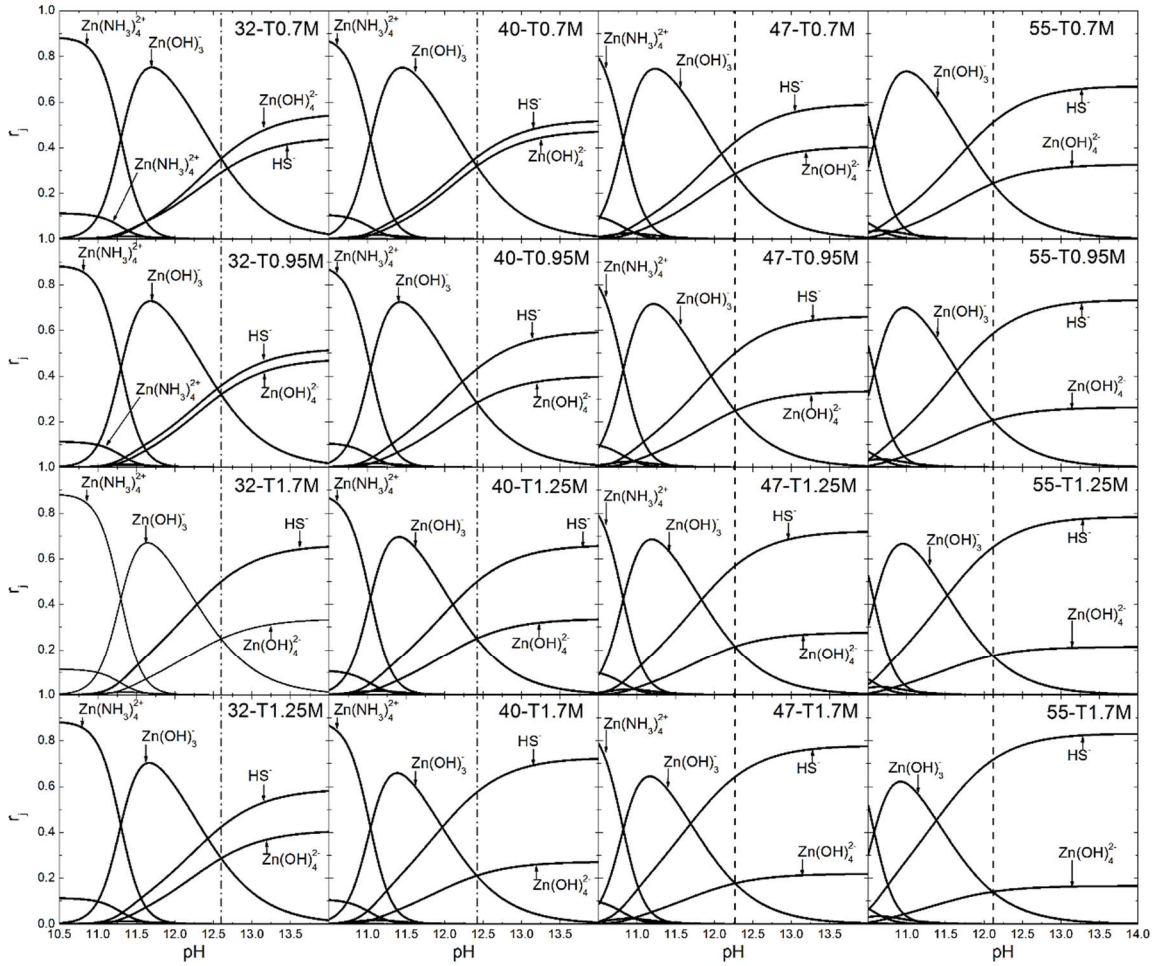

Figure 2.7. SDD at different temperatures and concentration of thiourea.

Table 2.3. *Proper chemical conditions for ZnS deposition at temperatures close to the ambient.*

Temperature (°C)	Thiourea concentration (M)	desired pH
25	2.25	12.77
32	1.70	12.60
40	1.25	12.42
47	0.95	12.25
55	0.70	12.10

CHAPTER 3

EXPERIMENTAL SET UP

In this chapter the methodology used to obtain ZnS thin films by the CBD technique is described. Afterwards, the method and instrumentation used to prepare the samples by means of the CBD technique will also be discussed. Finally, a brief description of the characterization techniques, that allowed obtain the morphological, chemical, structural and optical properties of the ZnS samples, is reviewed.

3.1. Experimental conditions

In order to experimentally demonstrate the different suitable conditions previously discussed, different groups of CBD-ZnS films were prepared. Table 3.1 shows the chemical conditions used to synthesize each group of ZnS films. The concentration of $ZnCl_2$ was of 0.02 M while the concentrations of KOH and NH_4NO_3 were varied until the pH value proposed in Table 2.3 was obtained.

Table 3.1. *Chemical conditions used for the CBD-ZnS films deposition.*

Temperature (°C)	Chemical reagents and concentrations (M)			
	$[SC(NH_2)_2]$	$[ZnCl_2]$	[KOH]	$[NH_4NO_3]$
25	2.25	0.02	1.0	1.5
32	1.95			
40	1.25			
47	0.95			
55	0.70			

The concentrations of zinc chloride and thiourea allow the ionic product to exceed the solubility product, while the concentrations of ammonium nitrate and potassium hydroxide permit the solution to obtain the desired pH value. For comparative purposes, non-proper conditions (lack of sulfur species) were obtained for temperatures of 25, 40 and 55 °C and the concentrations of such conditions are shown in Table 3.2

Table 3.2. *Non-proper chemical conditions used for the CBD-ZnS films deposition*

Temperature (°C)	Chemical reagents and concentrations (M)			
	$[ZnCl_2]$	[KOH]	$[NH_4NO_3]$	$[SC(NH_2)_2]$
25	0.02	1.0	1.5	1.10
40				0.64
55				0.35

3.2. Preparation of the chemical solution and samples deposition

The substrates used in the deposition process were of Corning glass whose commercial presentation is 25 mm x 75 mm with a thickness of 1.0 mm. The substrates are trimmed to obtain pieces of 15 x 25 mm^2 as deposition area. To achieve a greater adhesion between the film and the substrate, it is necessary that the glass substrate is as clean as possible. This is achieved by a strict cleaning process described below [30, 34]:

1. Wash the substrates with soap and water using a swab. Rinse them with plenty of distilled water and dry with compressed air.

2. Submerge the substrates in trichloroethylene within an ultrasonic bath for 5 min. Rinse them with plenty of distilled water and dry with compressed air.

3. Submerge the substrates in acetone in an ultrasonic bath for 5 min. Rinse them with plenty of distilled water and dry with compressed air.

4. Submerge the substrates in isopropyl alcohol in an ultrasonic bath for 5 min and dry them with compressed air.

The cleaned substrates are attached to substrate-holders made of Teflon in order to avoid chemical reactions between them and the bath solution. Finally, the substrates, already mounted on their substrate-holders, are vertically placed on an acrylic cap in a cylindrical glass crystallizer which contain the solution as is shown in Figure 3.1.

Figure 3.1. Substrates and substrate-holders assembly in the crystallizer containing the bath solution.

For preparing the bath solution it is necessary to dilute each reagent in distilled water as follows: $ZnCl_2$ in 80 mL, KOH in 200 mL, NH_4NO_3 in 80 mL and $SC(NH_2)_2$ in 80 mL. To obtain the bath solution, the reagents were mixed as follows: the $ZnCl_2$ solution is firstly added to the crystallizer, then the KOH solution followed by NH_4NO_3 and finally, the thiourea. The bath temperature of 25 °C corresponds to the controlled temperature of the laboratory where the experiments were carried out. For the other four temperatures, the bath solution was heated with a hot plate equipped with an electronic temperature controller with

an accuracy of ± 1 °C. For homogenization purposes, the chemical solution was permanently agitated with a magnetic stirrer at low velocity such that vorticities are avoided. During deposition, the pH of the solution was monitored with a pH-meter (OAKTON pH700). Figure 3.2 shows a photo of the implemented experimental system that allows obtaining the ZnS thin films by the CBD technique.

The deposition time begins when thiourea is added to the solution. In order to carry out a study according to the deposition time and temperature, each batch was formed of five samples, which were removed from the solution at different times. The deposition times for each temperature are shown in Table 3.3. For non-proper conditions, the deposition times used were the same as the used for experiments with proper conditions.

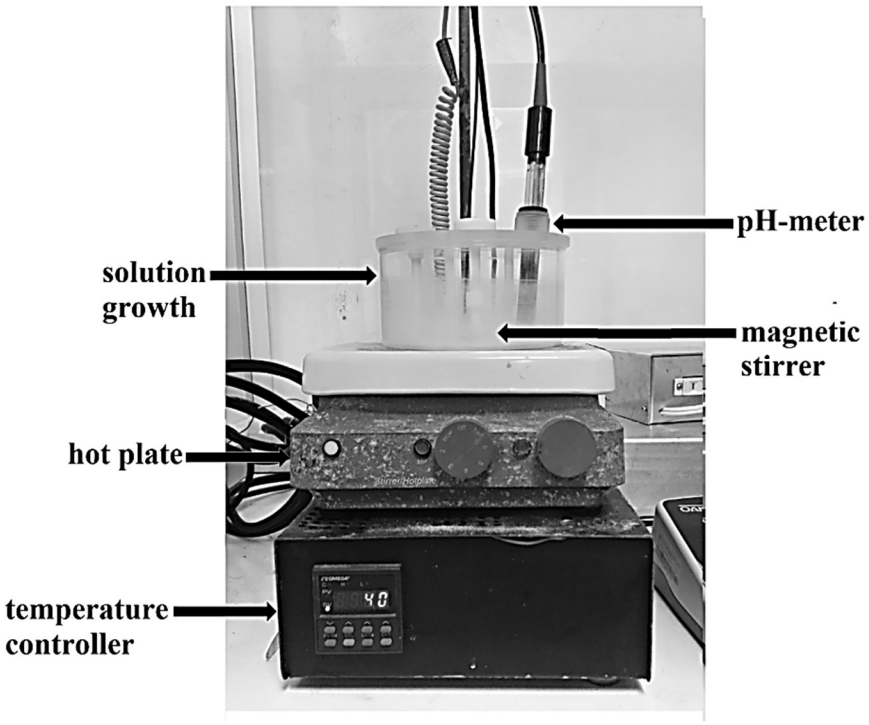

Figure 3.2. Experimental set up for obtaining the ZnS films by the CBD technique.

Table 3.3. *Deposition times for each prepared sample at different temperatures.*

Bath	Temperature (°C)	Deposition time (h)				
		Sample 1	Sample 2	Sample 3	Sample 4	Sample 5
1	25	24	48	72	96	120
2	32	20	32	44	56	68
3	40	15	20	25	30	35
4	47	8	12	16	20	24
5	55	3	5	7	9	11

After samples were removed from the solution, they were subject to a final cleaning process consisting of the following steps:

a) The samples were rinsed with distilled water and cleaned into an ultrasonic bath for 1 min to remove poor –adhered material.
b) Samples were dried at room temperature.
c) The film deposited on the opposite side of the substrate was removed with a 10% hydrochloric acid (HCl) solution with the aid of a cotton.
d) Samples were stored in a Petri-glass to ensure their shelter and avoid further contamination with the environment.

3.3. Characterization of the samples

After deposition, the films were characterized with different techniques for determining their morphological, chemical, structural, and optical properties.

3.3.1. Morphological characterization

3.3.1.1. Scanning electron microscope

Scanning electron microscope (SEM) generates a topographic image of a sample by the interaction of an electron beam that "scans" a certain area of the sample's surface. The technique consists of accelerated electrons with an average potential of 25 kV hitting on the surface of sample. When colliding with surface, different signals are released that, when captured with adequate sensors, provide information about the nature of the sample. One of these low energy emitted signals is called secondary electrons. Secondary electrons come from the analyzed sample and may be generated by collisions with the nucleus, where the loss of energy occurs or by the ejection of electrons weakly bound to the atoms in sample. The energy of the secondary electrons is typically 50 eV or less. An increase of detected secondary electrons causes an increase in the voltage of the detector and therefore in the intensity, which generates a brighter area in the image. If the beam encounters a depression in the sample, few electrons will be detected and therefore the intensity in the detector will be low also generating an opaque area in the image. The SEM image is formed of many points of different intensities depending on the captured voltage, which form the topography of sample as is shown in Figure 3.3. Samples with different deposition times of each bath temperature were analyzed with the SEM (JEOL 7600F) technique to obtain magnified images of its surface as a high as 50000x.

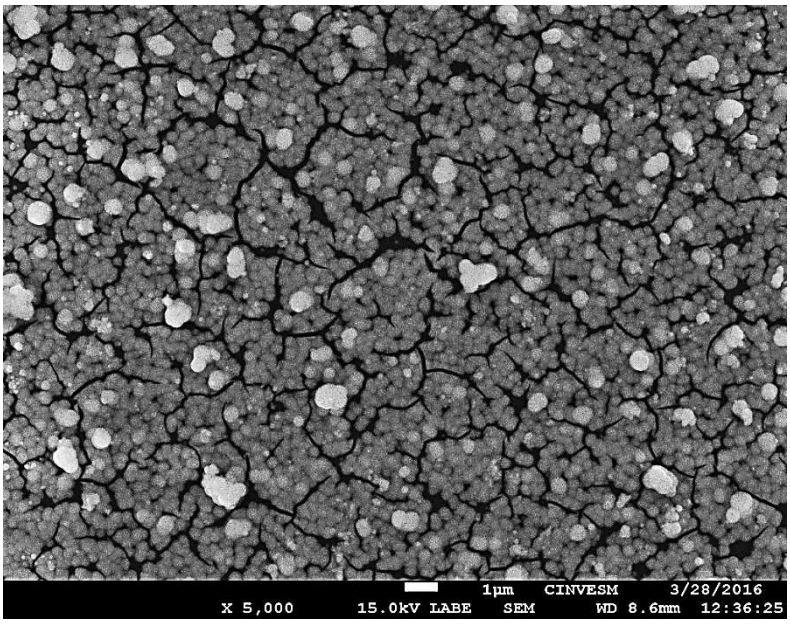

Figure 3.3. SEM image of the ZnS surface obtained by the CBD technique.

3.3.1.2. Profilometry

This technique allows measuring the thickness of thin films samples. The profilometer has a diamond tip in contact with the sample for scanning a formed step. The tip moves to the surface of the sample by applying a constant force on it where the scan-length varies according to the characteristics of the sample. The tip is connected to a measuring system that records the vertical displacements that it undergoes along the surface of the sample. For the measurement it is necessary that the sample has a step which serves as a reference between the substrate and the sample, as described in Figure 3.4. Unlike the Atomic force microscope (AFM), a profilometer has high resolution only in the vertical direction.

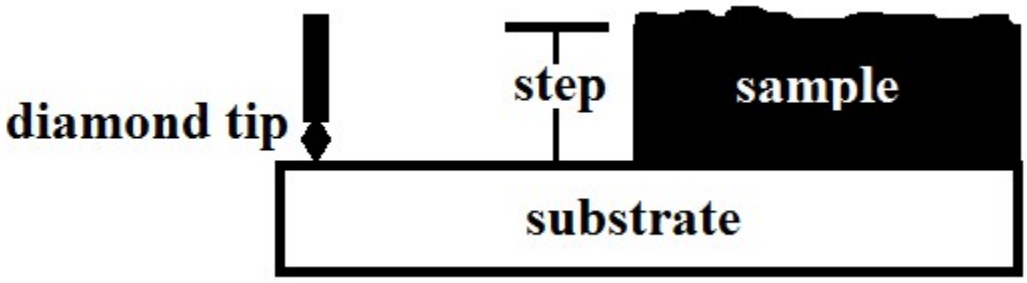

Figure 3.4. Schematic of a profilemeter.

Thickness of samples obtained with proper and no-proper conditions were analyzed with a DEKTAK 8 profilometer. The measurements in the profilometer allow obtaining the changes in thickness of the samples as a function of the deposition time. By a linear adjustment, the initial rate of growth (in nm/h) of this process, can be estimated by means of the slope of the straight line resulting from the adjustment.

3.3.2. Optical characterization by UV-VIS spectrophotometry

Ultraviolet and visible (UV-Vis) absorption spectrophotometry is the measurement of the attenuation (absorbed or transmitted) of a beam light after it passes through a sample. The signal can be used to determine the value of the bandgap energy (E_g) of semiconductors since it is related to the absorption coefficient (α) of the material by the equation [35]:

$$\alpha = A\left(h\nu - E_g\right)^n \tag{3.1}$$

where $h\nu$ is the energy of the incident photon on the sample (h is the Planck´s constant and ν is the photon frequency), A is a constant and the exponent n can take the value of 0.5 or 2 for an direct or an indirect band, respectively. ZnS is a crystalline material with a direct bandgap energy so exponent n will have a value of 0.5. The values of the absorption coefficient (α) are calculated by using the equation [36]:

$$I_t = I_0 e^{-\alpha d} \tag{3.2}$$

where d is the thickness of the film, and I_t and I_0 are the intensities of the transmitted and incident light, respectively. From Eq. (3.1) a linear relationship between α^2 and hv can be noted. When a plot of α^2 vs hv is done, the absorption line with intersection at $\alpha^2 = 0$ can be used to obtain the bandgap energy value of the material, this is, $hv=E_g$. In this technique, the wavelength is varied in a range of the electromagnetic spectrum comprising ultraviolet, visible and near infrared wavelengths (300-1100 nm) to analyze the variation of the absorption spectrum of the material. Absorption and transmission spectra of all samples were obtained with a spectrophotometer UV-VIS AE-UV1608PC in the 300-1100 nm wavelength range.

3.3.3. Chemical characterization by X-ray photoelectron spectroscopy

X-ray photoelectron spectroscopy (XPS), also known as electron spectroscopy for chemical analysis (ESCA) is the most widely used surface analysis technique applied to a broad range of materials to provide valuable quantitative and chemical state information from the surface of the materials of interest. When an atom or molecule absorbs an X-ray photon, an electron can be ejected. The kinetic energy (KE) of the electron depends upon the photon energy (hv) and the binding energy (BE) of the electron (i.e., the energy required to remove the electron from the surface). The equation governing this process is:

$$KE = hv - BE \tag{3.3}$$

By measuring the kinetic energy of the emitted electrons, it is possible to determine which elements are near the surface, their chemical states and the binding energy of the electrons. The binding energy depends upon a number of factors, including the following: the element from which the electron is emitted, the orbital from which the electron is ejected,

and the chemical environment of the atom from which the electron was emitted. XPS is a quantitative technique because the cross-section for the emission of a photoelectron is not dependent upon the chemical environment of the atom. XPS is typically accomplished by exciting a samples surface with mono-energetic Al Kα X-rays causing photoelectrons to be emitted from the sample surface. An electron energy analyzer is used to measure the energy of the emitted photoelectrons. From the binding energy and intensity of a photoelectron peak, the elemental identity, chemical state, and quantity of a detected element can be determined. X-ray photoelectron spectroscopy measurements were performed using a Thermo Scientific spectroscope with an Al-Kα source for the samples with the highest deposition times.

3.3.4. Structural characterization by X-ray diffraction

X-ray diffraction occurs when an X-ray beam interacts with a crystalline structure. When an X-ray beam with a specific wavelength of the same order of magnitude of the interatomic distances insides on the material, the X-rays are dispersed in all directions. Most of the radiation scattered by one atom overrides the radiation scattered in other atoms. However, X-rays that reach certain crystallographic planes forming specific angles with them are reinforced rather than annihilated. This is the diffraction phenomenon. X-rays are diffracted when conditions satisfy the Bragg's law:

$$2d_{hkl}Sen\theta = n\lambda \tag{3.4}$$

where the angle θ is the half of the angle formed by the diffracted beam and the original beam, λ is the wavelength of the incident x-rays and d_{hkl} is the interplanar distance that produces constructive reinforcement of the beam (Figure 3.5)

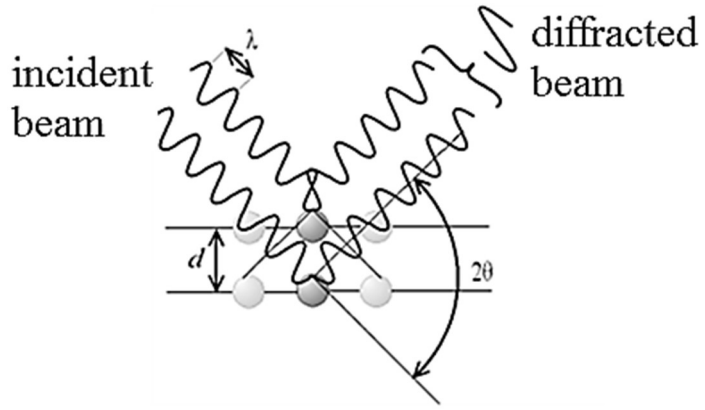

Figure 3.5. Diffraction phenomenon. Constructive interaction between X-rays and the crystalline material.

In a diffractometer a mobile X-ray detector records the angles *2θ* with which they are diffracted and a characteristic diffraction pattern is obtained. By knowing the wavelength of the x-rays (usually $\lambda_{CuK\alpha}$ = 1.5418 Å) it is possible to determine the distance between the planes; and finally, the identification of the planes that cause diffraction. There are various ways for determining the diffraction patterns of a material. For thin films*, grazing incidence* mode is used, which insides the X-ray beam at a very small angle (less than 1°) with respect to the surface of sample due to the thickness of the sample. The planes that satisfy the Bragg's law will give constructive signals. The crystalline structure of the samples with the highest deposition times were investigated by using an X-ray diffractometer Siemens D-5000 at grazing incidence of 0.5°.

CHAPTER 4

RESULTS OF THE KINETIC STUDY

4.1. Dynamic evolution of the growth of the films

In a typical process of growing of any material by the CBD technique, three stages are present during all the deposition time. The first stage, called the *induction zone*, is the period where there is no growth of the material given the formation of the first nuclei of growth; in the second stage, known as *growing zone,* the material grows on substrate producing an increase in the film thickness; finally, the *saturation zone* wherein the growth of the material finishes or decreases due to a reduction or depletion of the reactants [28]. For the ZnS, these three stages can be experimentally observed through the cloudy or clarity of the chemical solution. In the *induction zone,* a transparent solution is normally observed. During the *growing zone* the solution becomes opaque with a whitish coloration indicating the presence of the precipitates. Finally, a more opaque tone (cloudy) is observed in the *saturation zone* where the growth of film finalizes.

Figure 4.1 shows the evolution of the thickness of the ZnS film as a function of the deposition time and bath temperature. At 25 °C, no deposition of ZnS material was observed onto the substrates during the first 24 h (*induction zone*). For the time interval between 24 and 120 h (*growing zone*), an increase on the thickness was observed, up to a value of 113 nm. By assuming a linear behavior in the *growing zone*, the growth rate value (the slope) of the ZnS film in this case, was estimated as 1.3 nm/h.

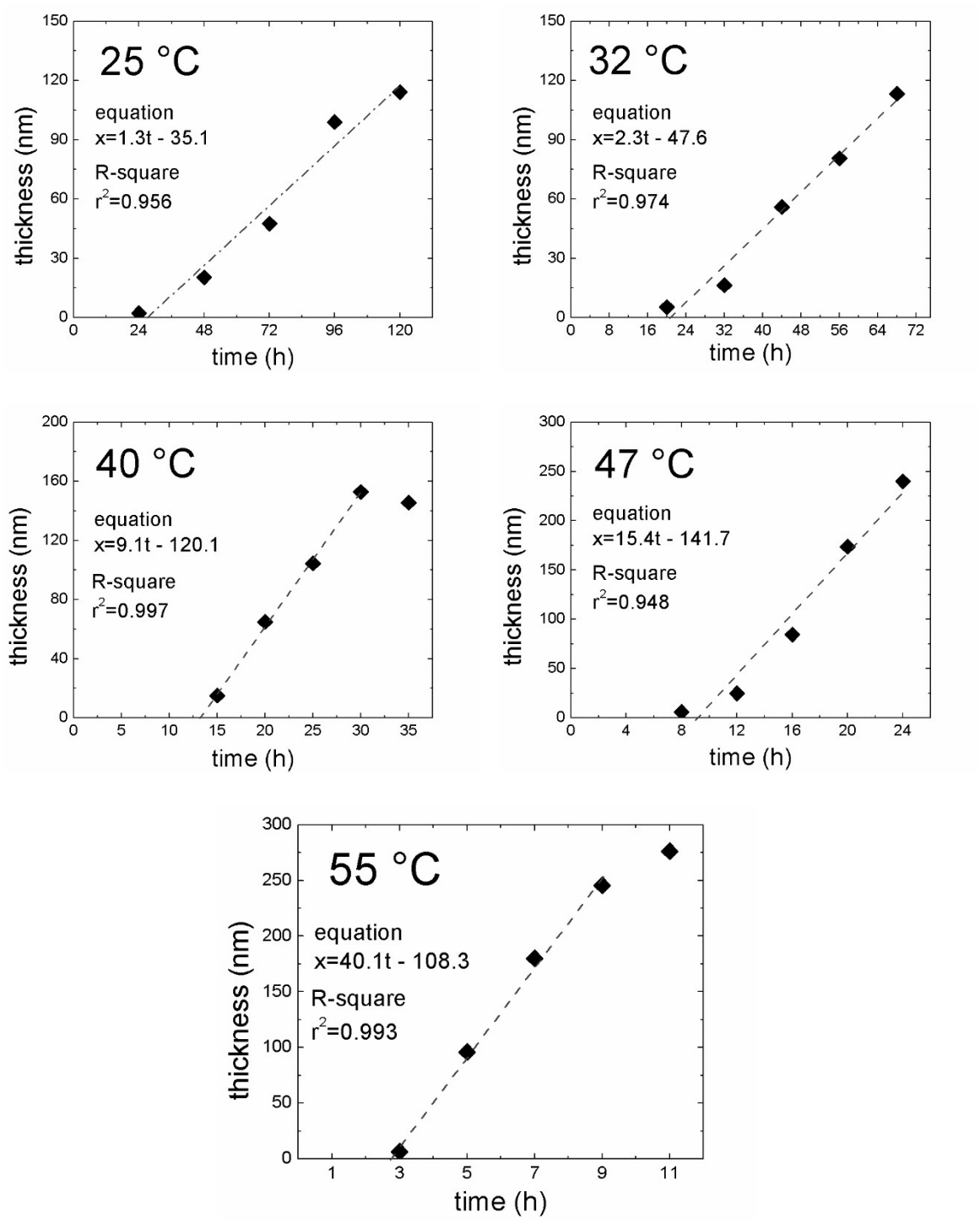

Figure 4.1. Evolution of the ZnS film thickness (x) as a function of the deposition time (t) for different temperatures of the chemical solution.

By increasing the temperature of the chemical bath at 32 °C, the *induction zone* becomes slightly shorter (20 h) as compared to the bath at 25 °C (24 h). This indicates that the deposition of ZnS started sooner at 32 °C. For deposition times above 20 h, an increasing behavior of the thickness was registered until 66 h, where a maximum thickness of 115 nm was measured. By assuming a linear increasing behavior, the growth rate at 32 °C was estimated at 2.3 nm/h. For the bath temperature of 40 °C, the time of the *induction zone* was diminished to 13 h and, for longer times, the thickness continuously increased up to 30 h, where a maximum thickness of 153 nm was achieved with an estimated rate of growth of 9.1 nm/h. For deposition times above 30 h, no increase of the thickness of ZnS film was observed (*saturation zone*).

For the chemical baths prepared at 47 °C and 55 °C, the shortest times of the *induction zone* were registered, whose values were estimated as 7 h and 3 h, respectively. At 47 °C, a maximum thickness of 240 nm with a growth rate of 15.4 nm/h were obtained, meanwhile at 55 °C a maximum thickness of 276 nm with a growth rate of 40.1 nm/h were estimated. It is evident that there exist an exponential behavior between the growth rate of the material and the bath temperature, whereby it can be concluded that higher temperatures in the chemical bath promote faster formation of ZnS and higher thicknesses in the formed film. Thus, it can be assumed that temperature provides enough thermal energy to the reactants, inducing them for easy dissociation; as a consequence, the resulting ions react more easily between them to form nuclei and to accelerate the growing process.

4.2. Dynamic evolution of the film thickness: effect of the thiourea concentration

From the physicochemical analysis detailed in Chapter 2, we discussed the necessity for using adequate concentrations of thiourea to ensure a proper growth of the ZnS film. In

order to study these effects on the ZnS films when the concentration of thiourea is not proper, samples were synthesized with conditions listed in Table 3.2. Figure 4.2 shows the evolution of the film thickness as a function of deposition time and temperature for these conditions.

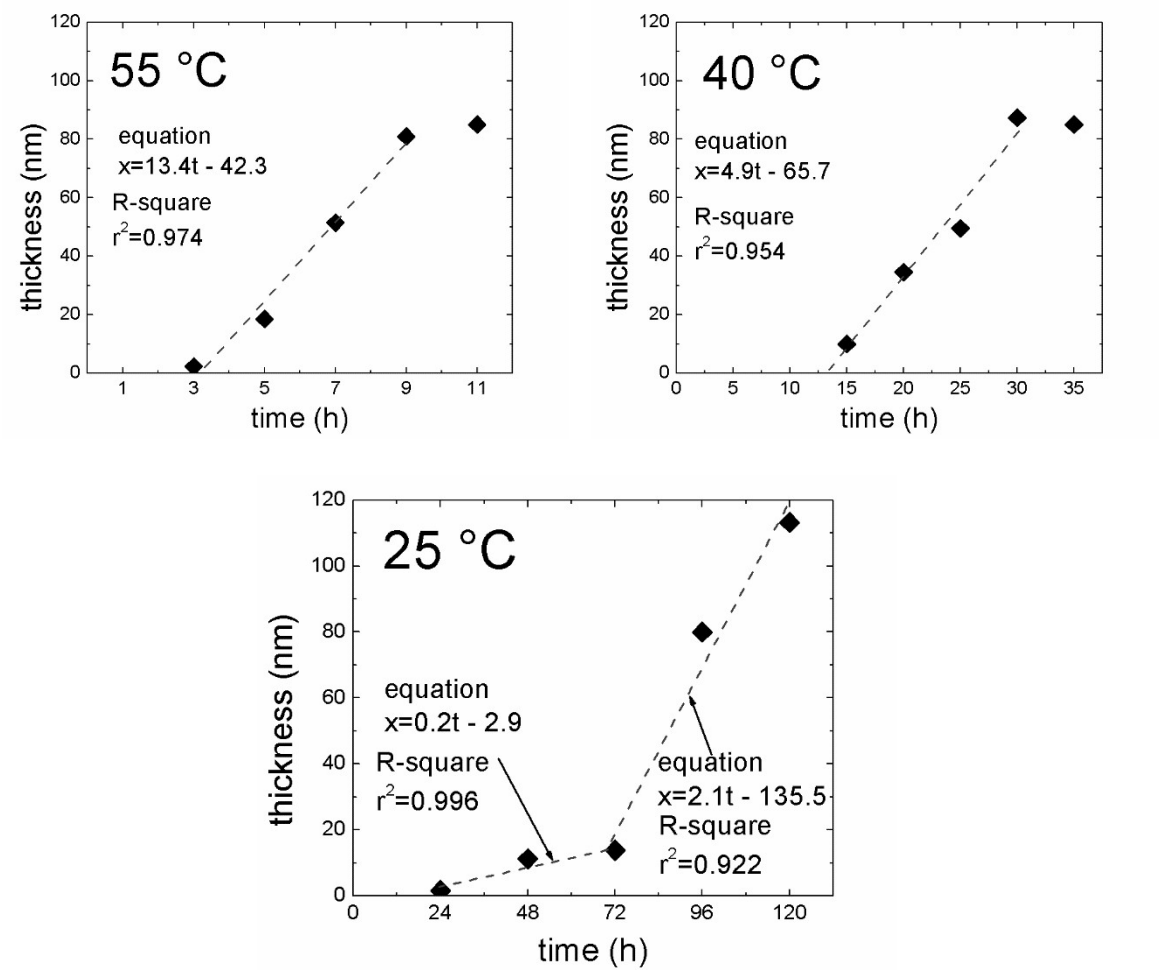

Figure. 4.2 Evolution of the ZnS film thickness (x) as a function of the deposition time (t) for non-proper growth conditions.

The behavior of thickness as a function of deposition time can be seen in Figure 4.2, where not significant changes with respect to the proper conditions are observed. The times of the *induction* and *growing zones* seem similar to the obtained under proper conditions, and only a slightly increase of the induction time was observed in comparison to the results

discussed in Figure 4.1. However, noticeable changes in the maximum thickness and rate of growth can be highlighted. The rate of growth was reduced from 9.1 to 4.9 nm/h when the bath temperature is of 40 °C and from 40.1 to 13.4 nm/h when it is of 55 °C. As a consequence of these low rates of growth, the maximum thickness reached for each temperature is also decreased, reducing its value from 153 to 87 nm for 40 °C, and from 276 to 85 nm for 55 °C. When the bath temperature is 25 °C, a change in the rate of growth of the material in the *growing zone* can be observed, changing from 0.2 nm/h to 2.1 nm/h after 72 h of deposition. This change in the rate of growth can be explained by the changes in the growth mechanism. Despite this, the maximum thickness of film does not change radically, with a slightly increase toward 118 nm in comparison with the 113 nm value achieved with the proper concentration of thiourea. Thus, it can be concluded that the insufficiency of HS^- ions in the solution decelerates the growth of the material since the stoichiometry of Eq. (2.23) is altered, causing a reduction of ZnS as a product.

4.3. Evolution of pH of the chemical bath

Figure 4.3 shows the evolution of the measured pH in the chemical solution as a function of the deposition time for the proper growth conditions. A slight difference between the initial pH value (0 h) and the final pH value (maximum deposition time) for the temperatures of 55, 47, and 40 °C, can be observed, such that a constant pH value throughout the deposition time can be considered. When the bath temperature is 32 °C, the pH shows a similar initial behavior to that of the higher temperatures, since it remains constant for 44 h with a slightly decrease at the end of the deposition time. At this temperature the change between the initial and final pH is more significant than for 40, 47 and 55 °C. The bath solution carried out at 25 °C shows a different behavior. It shows a pronounced drop of ΔpH

= 0.4 during the first 24 h of deposition and a plateau around pH = 12.77 for the remainder of the time. As the temperature of the solution increases, the ΔpH value decreases from 0.5 when the temperature is 25 °C to 0.03 for a temperature of 55 °C.

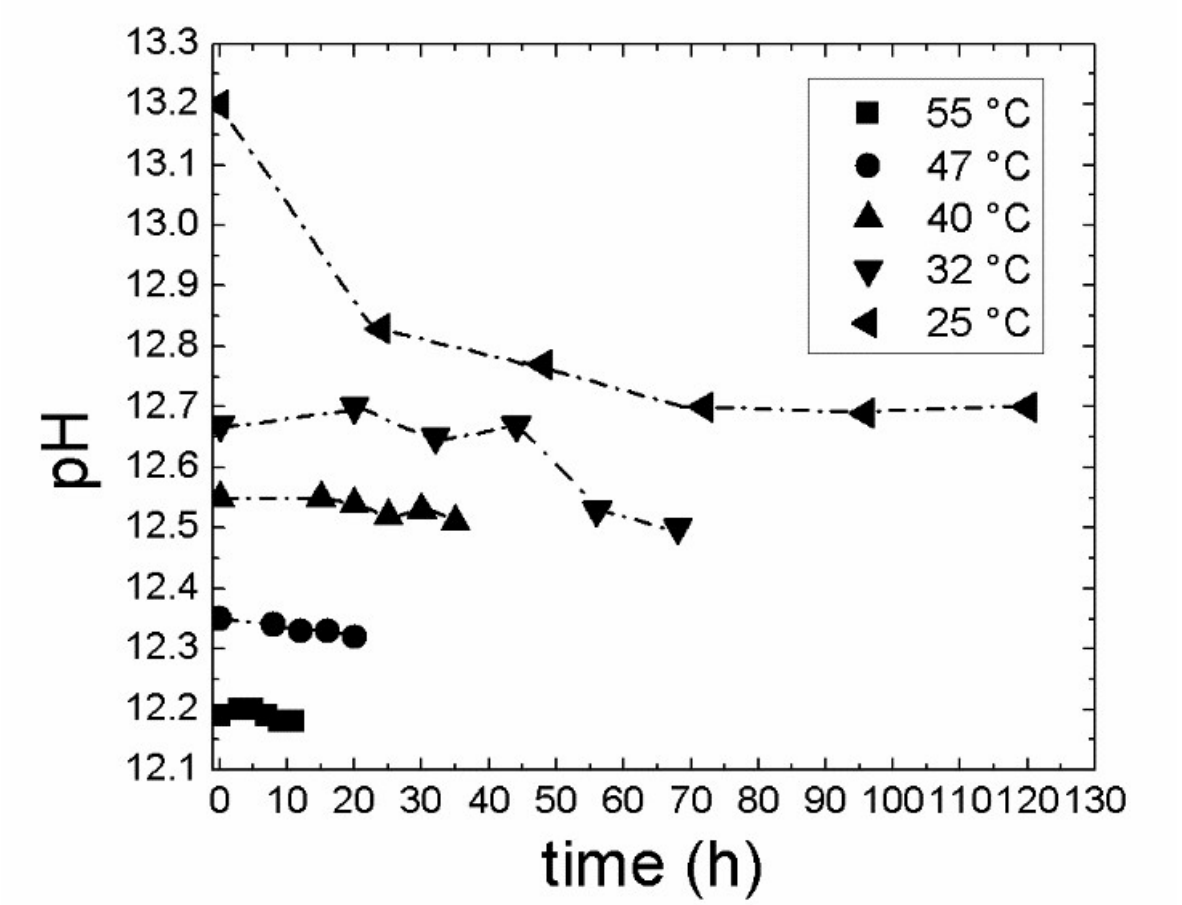

Figure. 4.3. pH of the chemical bath as a function of the deposition time for different temperatures.

Figure 4.4 shows the pH evolution of the solution for the non-proper ZnS growth conditions. It can be seen that when the bath temperature are 55 °C and o 40 °C there is a small change in the behavior of the pH compared to the appropriate conditions. The change of pH for these conditions is greater than the obtained when the concentration of thiourea is adequate, increasing from 0.03 to 0.09 for 55 °C and from 0.04 to 0.14 for 40 °C. At 25 °C

this change in pH is higher, showing an important decrease during the first 72 h of the experiment with the proper condition; however, after this time, the pH of the solution shows a continuous decrease until a value of pH = 11.9, which with the proper conditions is not observed.

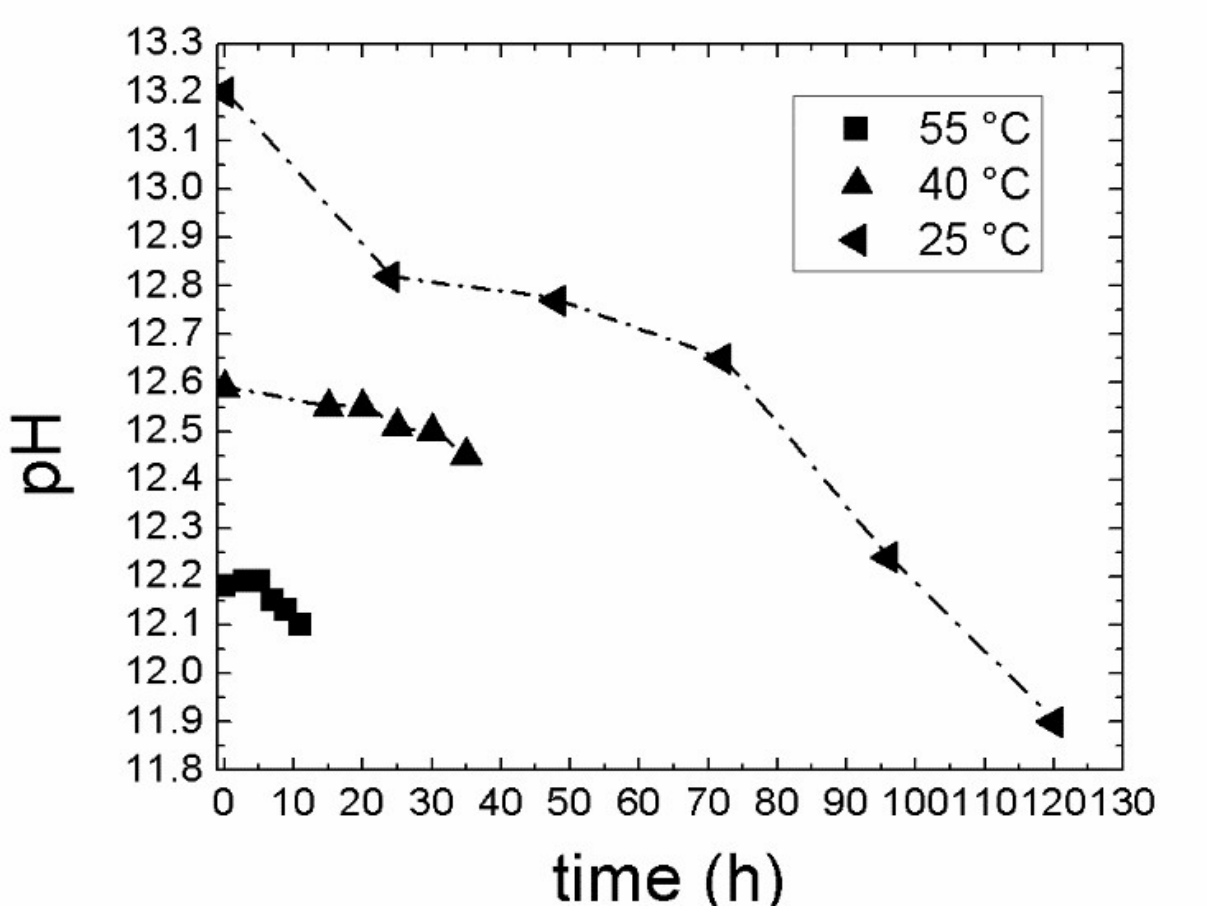

Figure 4.4. pH of the chemical bath as a function of the deposition time for different temperatures with non-proper conditions.

4.4. Kinetic parameters

According to the results obtained in Section 4.1, a clear dependence between the growth rate of the material and the temperature of the bath is clearly observed. This behavior was demonstrated by Svante Arrhenius in 1888 [37]. According to his observations, the

molecules in a solution must possess some minimum amount of energy to react, a value that he called activation energy (E_a). Arrhenius determined that the increase of the growth rate with temperature is exponential. These observations were incorporated in a known classic equation (Arrhenius equation):

$$k(T) = Ae^{-\frac{E_a}{RT}} \tag{4.1}$$

In this equation, k is the temperature-dependent constant rate, E_a is the activation energy, R is the gas general constant (8.314 J/mol·K), T is the absolute temperature and A is a constant value related to the collisions between molecules. On the other hand, the growth rate of the material (v) also depends on the concentrations of the reactants, which are related by means of the following rate law equation [20, 28]:

$$v = k(T)[ZnCl_2]^{\alpha}[KOH]^{\beta}[NH_4NO_3]^{\gamma}[SC(NH_2)_2]^{\delta} \tag{4.2}$$

where α, β, γ and δ are the orders of the reaction for each chemical reagents. By substituting Eq. (4.1) in Eq. (4.2) can be obtained the global equation of the ZnS growth rate:

$$v = Ae^{-\frac{E_a}{RT}}[ZnCl_2]^{\alpha}[KOH]^{\beta}[NH_4NO_3]^{\gamma}[SC(NH_2)_2]^{\delta} \tag{4.3}$$

If for given conditions, the growth rate depends only on a certain reagent concentration, in this case the thiourea, Eq. (4.3) can be expressed as follows:

$$v = Be^{-\frac{E_a}{RT}}[SC(NH_2)_2]^{\delta} \tag{4.4}$$

where B is a constant that incorporates the concentrations of the remainder of the reactants. In order to determinate the dependence of the growth rate with the initial concentration of the thiourea, the method of the initial rates was used [20, 29]. Note that Eq. (4.4) would have

a linear behavior if the natural logarithm function is applied in both sides of such equation. This operation permits to obtain:

$$\ln v = \ln B - \frac{E_a}{R}\left(\frac{1}{T}\right) + \delta \ln[SC(NH_2)_2] \quad (4.5)$$

The activation energy of the system and the thiourea-dependent reaction order can be obtained with Eq. (4.5) by applying a multilineal regression and taking into account the data provided in Table 4.1.

Table 4.1. *Used data for the multilineal regression*

ln *v*	**(1/T) (K^{-1})**	**ln [$SC(NH_2)_2$]**
3.690	0.00305	-0.35667
2.736	0.00313	-0.05129
2.204	0.00319	0.22314
0.811	0.00328	0.53063
0.285	0.00336	0.81093

From the multilineal regression is obtained:

$$\ln v = 50.62 - 15280.63\left(\frac{1}{T}\right) + 1.03 \ln[SC(NH_2)_2] \quad (4.6)$$

By comparing Eqs. (4.5) and (4.6) it is observed that the factor ($-E_a/R$) has a value of -15280.63, such that when the activation energy it is released, reaches a value of 127 ± 5 kJ/mol. Additionally, the order of the reaction (δ) for thiourea gives a value of 1.03 ± 0.05. These two values (E_a and δ) give a guideline about the interpretation of the growth mechanism of the material. From previous works in the literature, a comparison was done between the E_a values obtained by different research groups and the value obtained in this

work. Table 4.2 shows the values of these two parameters obtained by several previously published research groups.

Table 4.2. *Conditions and E_a values reported by other groups and its comparison with the value obtained in this work.*

Reference	System	Temperature range (°C)	Activation energy kJ/mol	Reaction order
[20]	$Zn^{2+}/NH_3/N_2H_4/SC(NH_2)_2$	60 - 90	20.9	---
[27]	$Zn^{2+}/NH_3/ SC(NH_2)_2$	60 – 90	32	---
[28]	$Zn^{2+}/NH_3/OH^-/SC(NH_2)_2$	60 – 90	58.9	1.2
[29]	$Zn^{2+}/NH_3/Na_3C_6H_5O_7/SC(NH_2)_2$	50 – 80	33.60	0.8
[30]	$Zn^{2+}/OH^-/NH_3/SC(NH_2)_2$	60 – 90	44.9	0
[38]	$Zn^{2+}/NH_3/ C_2H_5NS$	30 – 80	10.46	---
[39]	$Zn^{2+}/NH_3/N_2H_4/SC(NH_2)_2$	50 – 90	34-97	---
[40]	$Zn^{2+}/NH_3/ C_2H_6OS/SC(NH_2)_2$	60 – 90	60 - 100	---
This work	$Zn^{2+}/OH^-/NH_3/SC(NH_2)_2$	25 – 55	127	1.03

From Table 4.2 it can be noted that there is not a unique value for the activation energy, given its dependence with the chemical reagents and the temperature used for the growth of film. However, for growing the ZnS at reduced temperatures, energy requirements are much higher than for high temperatures because of, as mentioned above, the temperature promotes the dissociation of the reactants causing an increase in the formation of nuclei of growth and therefore, an increase in the rate of growth.

Traditionally, when the activation energy presents small values (E_a < 35 kJ/mol), the growth mechanism is attached to a physical process such as diffusion or adsorption, and is commonly called a homogeneous mechanism [41]. In this case, the zinc and the sulfur ions react between them without a complexing agent. This combination of ions takes place into the solution when the first clusters of ZnS are formed, which diffuse through the solution until reaching the surface of substrate where they are adsorbed. By an aggregation process, clusters combine with others to form the ZnS film. On the other hand, when the activation energy is high (E_a > 35 kJ/mol) the growth mechanism is normally explained by a chemical process called heterogeneous mechanism [42]. In this process, the formation of a zinc complexing ion is required, which will subsequently be adsorbed on the surface of the substrate. Once the complex ion has been adsorbed, an exchange reaction will be carried out with the sulfur ions to form the first nuclei of ZnS, a process called nucleophilic attack from a nearby anion. This process usually presents a chemical limitation that involves the relaxation of some bond or the decomposition of some chemical reagent [43]. The high value of 127 kJ/mol for the activation energy calculated for the CBD films deposited at temperatures close to the ambient temperature suggests that the growth mechanism of the ZnS is of heterogeneous type. Then, the formation of some complexing agents and the chemical reaction between the zinc complex and the sulfur species must be considered in the growth mechanism. On the other hand, the order of reaction different than zero indicates that there exists a clear dependence between the rate of growth and the concentration of thiourea. The dependence of the growth rate with reaction orders indicates that formation of the material is limited by some processes involving the thiourea [44].

CHAPTER 5

CHARACTERIZATION RESULTS

5.1. Chemical characterization by X-ray photoelectron spectroscopy

The chemical composition of the samples was obtained by X-ray photoelectron spectroscopy (XPS). The spectra of the zinc element were obtained for samples prepared with the longest deposition time for both proper and non-proper conditions. Figure 5.1 shows high resolution spectrum of zinc 2p correspond to the samples with proper conditions. Dashed lines indicate the binding energies attributed to the Zn-OH and Zn-S bonds positioned at 1021.5 and 1022.1 eV, respectively [45]. For proper concentrations of thiourea at 25, 32 and 40 °C, the main peak is centered between the two zinc bonding signals. For samples deposited at 47 and 55 °C, the peak is centered in the Zn-S bond. The deconvoluted signals show that the deposited films is formed by a mixture of ZnS and a certain amount of oxygen in the form of $Zn(OH)_2$ which decreases in intensity as the deposition temperature increases. Figure 5.2 shows the spectra of zinc for samples prepared under non-proper conditions. In these samples the main XPS peak is centered on the Zn-OH bond side and the deconvolution signals show a greater presence of oxygen (Zn-OH signal) than the sulfur (Zn-S) at temperatures of 25 and 40 °C. At 55 °C, unlike the spectrum with proper conditions where the Zn-OH signal is almost null, with non-proper conditions the zinc binds with both sulfur and hydroxide ions, but with more Zn-S ligands than Zn-OH compared to the other non-proper conditions.

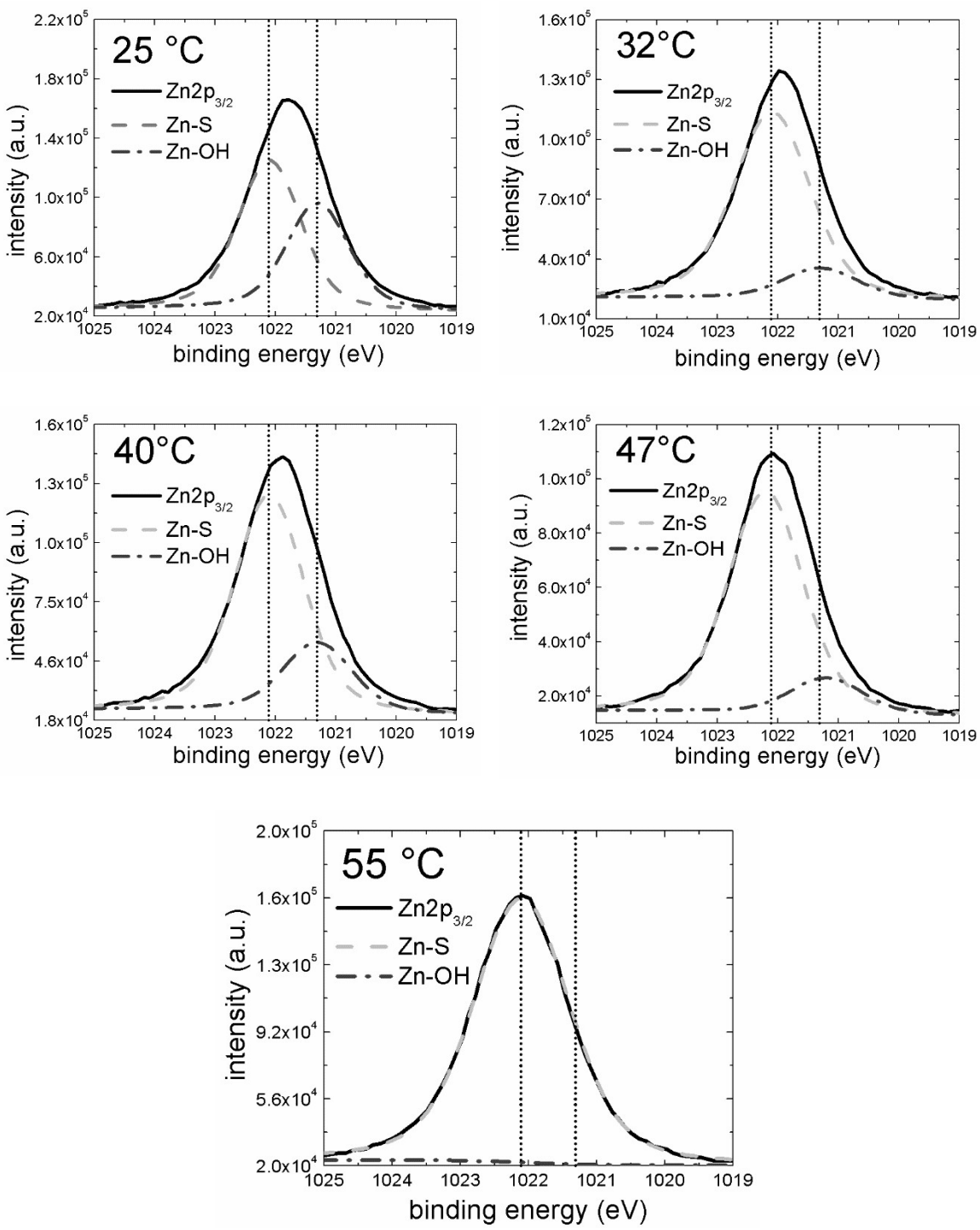

Figure 5.1. XPS spectra of zinc for samples grown with proper thiourea concentrations.

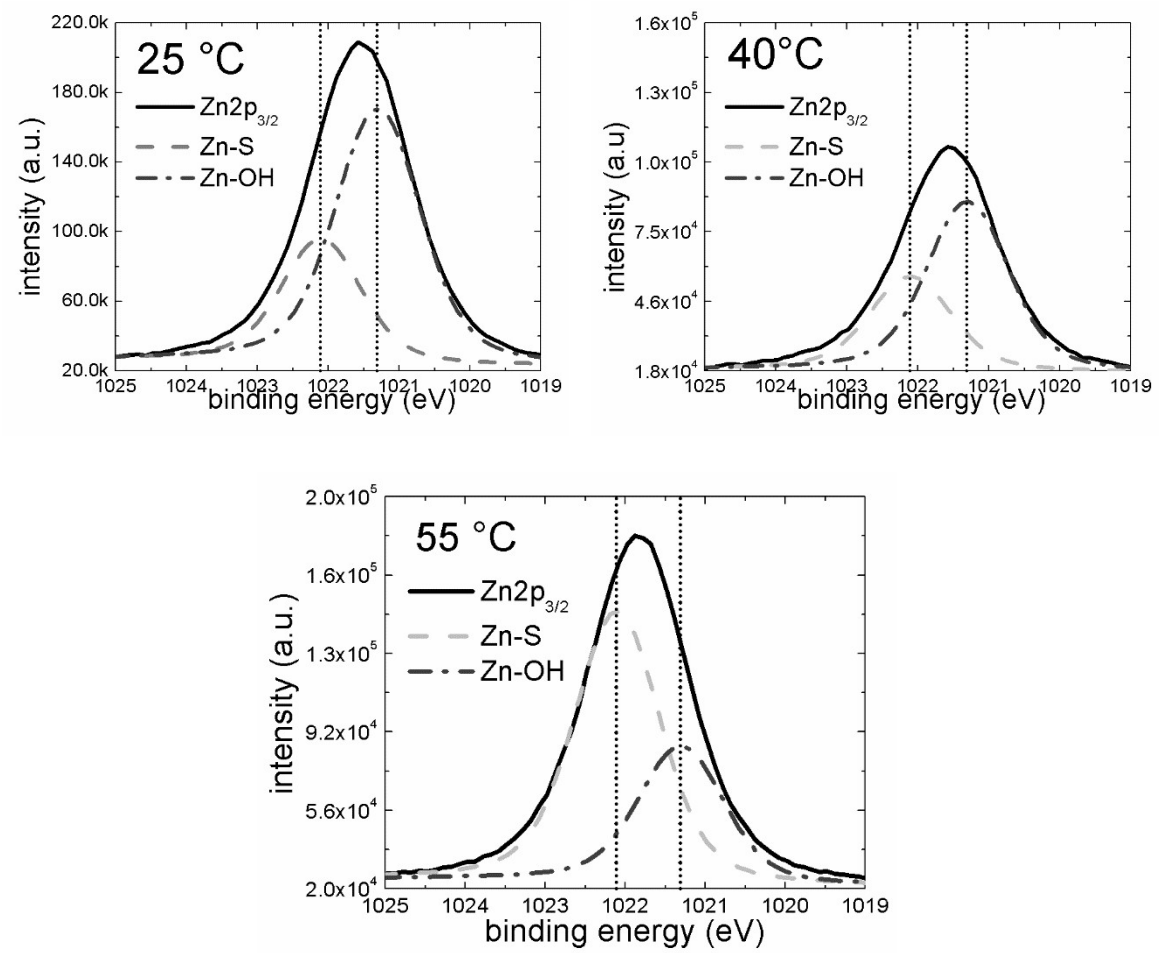

Figure 5.2. XPS spectra of zinc for samples grown with non-proper thiourea concentrations.

The peak area ratio (ε) is defined as [46]:

$$\varepsilon = \frac{I_{ZnS}}{I_{ZnS}+I_{ZnOH}} \tag{5.1}$$

where I_{ZnS} and I_{ZnOH} are the deconvoluted peak areas of the Zn-S and Zn-OH bonds, respectively. Ratio ε provides the percentage of zinc bounded to sulfur (as ZnS). Calculations of the ε ratio and the elemental atomic concentrations are shown in Table 5.1.

Table 5.1. *Atomic concentration of the chemical bonds of the ZnS films deposited under different conditions.*

Sample		*atomic concentration (%)*		*concentration ratio*	Peak area ratio (ε)
		Zn	S	Zn/S	
Proper conditions	55°C	29.55	32.6	0.906	0.969
	47°C	26.32	31.62	0.832	0.853
	40°C	16.87	34.99	0.482	0.753
	32°C	15.57	29.84	0.521	0.773
	25°C	14.65	39.85	0.367	0.581
Non-proper conditions	55°C	20.44	40.46	0.505	0.662
	40°C	6.62	19.86	0.300	0.354
	25°C	3.88	17.29	0.224	0.306

For samples with proper conditions, the amount of zinc increases, meanwhile the sulfur concentration remains constant with the increase of temperature. The atomic concentration Zn/S ratio tends to be 1 (ideal stoichiometry) by increasing the temperature value, which indicates an improvement in the formation of ZnS only. For samples deposited with non-proper conditions the Zn/S ratio decreases as the deposition temperature is reduced. Note that the Zn/S ratio is much smaller than the ratio obtained with proper concentrations of thiourea. The value of ε ratio shows that despite having the proper concentration of thiourea, formation of $Zn(OH)_2$ at low temperatures cannot be avoided. These results validate the mentioned proposal for the growth mechanism: first, the dependence of the exchange reaction between the HS^- and OH^- ions with temperature and second, if there is not enough amount of HS^- ions in the growth solution, a double phase (between ZnS and $Zn(OH)_2$) will

be obtained in films. However, because the aqueous nature of the chemical bath technique, it results difficult to avoid the oxygen in the samples [47].

5.2. Structural characterization by X-ray diffraction technique

Figure 5.3 shows the results of the crystalline structure of the deposited ZnS films at a) proper and b) non-proper conditions, which was investigated by the X-ray diffraction (XRD) technique. The XRD spectra of the samples deposited at 55 °C and 47 °C with proper conditions show small diffraction peaks corresponding to the (100) orientation of the zinc blende structure detected at $2\theta \approx 28.5°$; additionally, the sample deposited at 55 °C presents an additional (220) peak of this structure [JCPDS 05-0566]. The other samples seem predominantly amorphous implying that these samples contain layers with small grains [48]. For samples obtained at 25 °C, two peaks related with $Zn(OH)_2$ at $2\theta \approx 22.2°$ for proper conditions, and $2\theta \approx 36.2°$ for non-proper conditions are obtained. These two small peaks indicate the presence of $Zn(OH)_2$ in samples as an orthorhombic structure. These results are in concordance with those obtained in the chemical characterization. Samples deposited at 55 °C and 47 °C are mainly formed by ZnS and possess better stoichiometry according to the ε ratio and the atomic concentration values, while for samples obtained at 25 °C present lower values indicating higher presence of $Zn(OH)_2$ than ZnS. Additionally, for temperatures closely to the ambient (25 to 40 °C), these conditions cannot provide enough energy for crystallization [49] and amorphous samples are expected. Last results show that crystalline structure on samples depends strongly on the bath temperature, since no thiourea concentration enhances the formation of any crystalline structure.

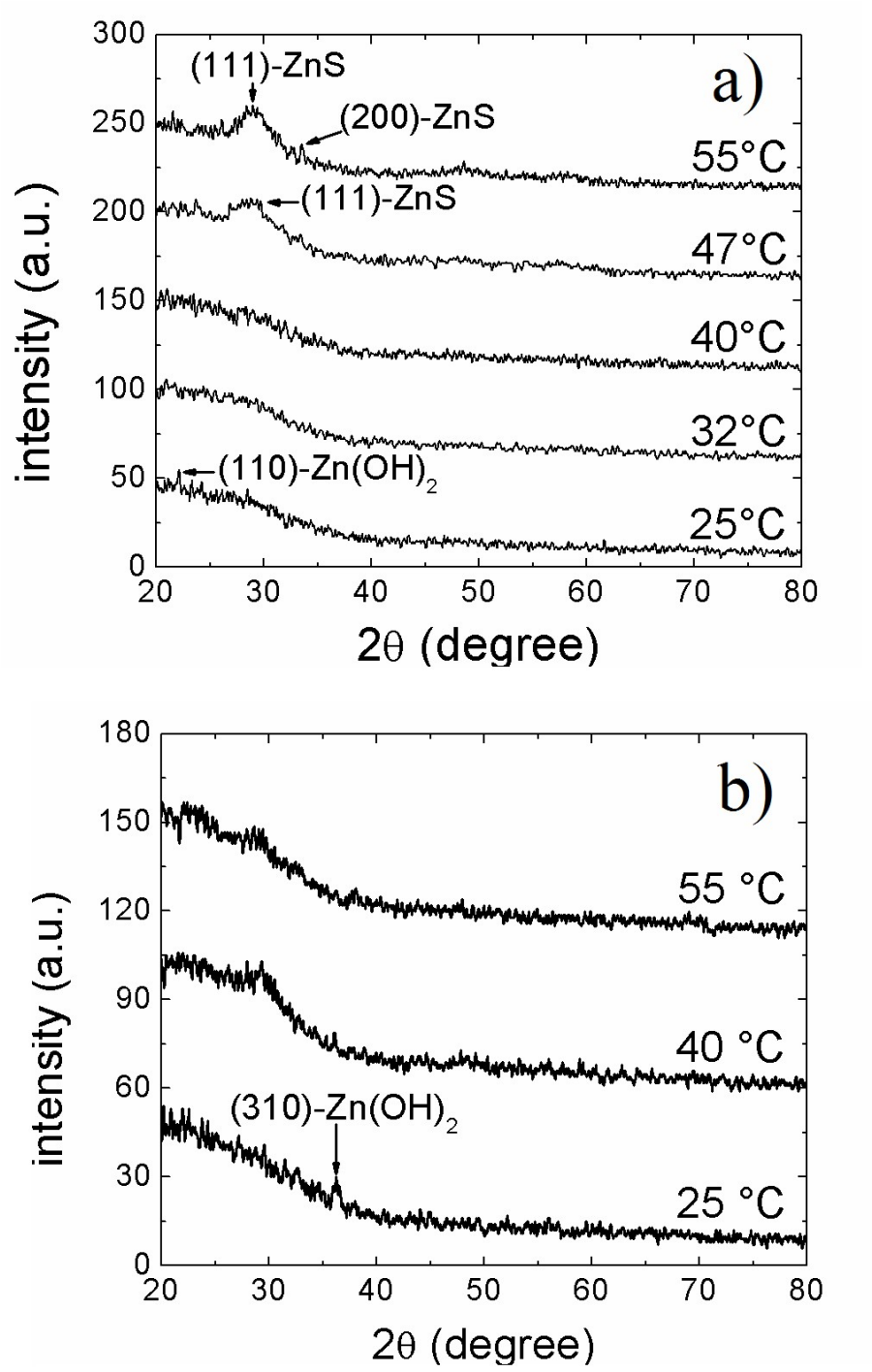

Figure 5.3 X-ray diffractograms for films with longer deposition time for: a) proper, and b) non-proper conditions.

5.3. Morphology characterization

The morphology of the ZnS films was investigated by scanning electronic microscope (SEM). For each temperature, three deposited films (the first, third, and fifth extracted samples) were analyzed. Figure 5.4 shows the SEM images of the ZnS films magnified 50000 times. By considering the deposition time, a clearly growth evolution of the grains is observed on the surface of the samples. For example, at 25 °C, the first sample (named 25-M1) corresponds to a deposition time of 24 h. This sample has barely exceeded the *induction time*, so that some particles appear as aggregates for the initial growth of the material. As the deposition time increases, the number of particles increases, making the surface of the material denser (25-M3). In a similar way, an increase on the size of the particles can be observed with time. The later deposited sample (25-M5), corresponding to the final part of the growth zone, is the sample with more density of particles on surface for this temperature. The surface seems completely filled with spherical particles, which is typical of the ZnS growth [50]. The effect of temperature can be observed by comparing the size of the particles for the same growth zone (columns in Figure 5.4). A notable growth in the size of agglomerates as the temperature increases is clearly observed, resulting in larger and better distributed particles in substrate producing a denser surface. This behavior reinforces the results obtained in the kinetic analysis. According to these results, an increase of deposition temperature causes that species reacts easily, producing, as a consequence, an increase in the deposition rate and denser and larger particles.

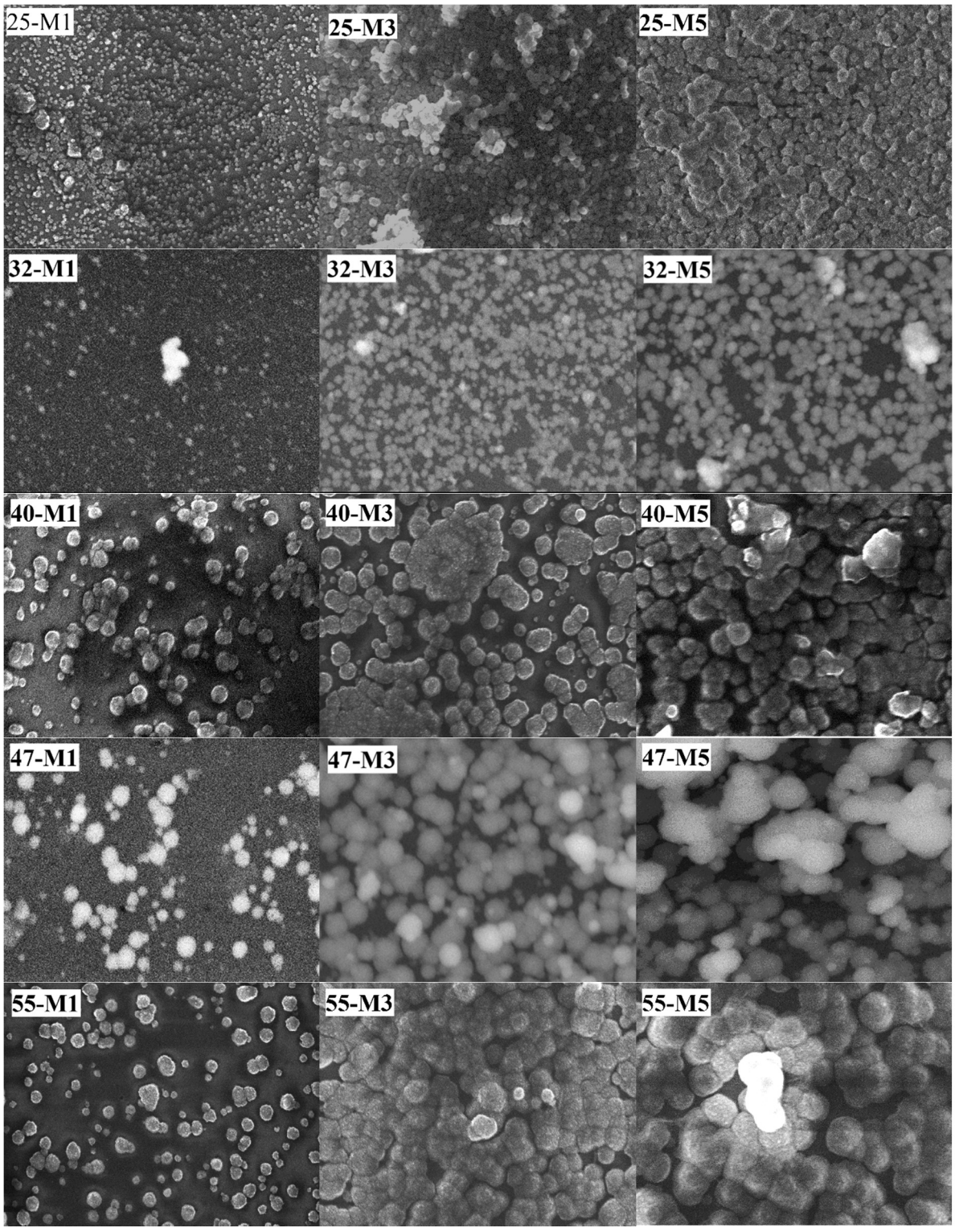

Figure 5.4. SEM images (50000x) of the samples as obtained for different deposition times for proper thiourea concentrations.

When the thiourea concentration is no proper, a change in the surface of the samples can be observed (Figure 5.5). At 55 °C and 40 °C, the analyzed surface of samples contains fewer particles than its grown counterparts prepared with proper conditions. The size of the particles is similar; however, they do not form a uniform layer and certain areas with small clumps of material can be seen. This effect on surface is due to the fact that when the concentration of thiourea decreases, the growth process is difficult because there is not enough HS^- ions in the solution, causing a lower rate of growth. For the samples deposited at 25 °C, the changes in surface are more noticeable. Although the first two samples (25-NP-M1 and 25-NP-M3) have similar surface area than their proper conditions counterparts, the last sample (25-NP-M5) does not present a uniform surface and the particle size varies greatly with a not well-defined shape of grains. This abrupt change in the surface of the material can be due to the reduction of pH of the solution, causing a higher formation of $Zn(OH)_2$ than of ZnS which is in concordance with the change of slope during the growth (Figure 4.2) and the results obtained of the chemical composition. A SEM image with 10000x magnification of the sample with longer deposition time prepared at 25 °C, can be seen in Figure 5.6. Sample prepared with non-proper conditions (25-NP) shows homogeneous surface with some particles randomly distributed on the surface. However, bigger particles tube-like with thorns is superimposed on the surface. A chemical analysis of these particles revealed the presence of Zn and O but not S. This confirms the mentioned considerations of the physicochemical and kinetic analysis. By adjusting the proper concentration of thiourea, these particles do not appear, but surface sample remains inhomogeneous (25-P).

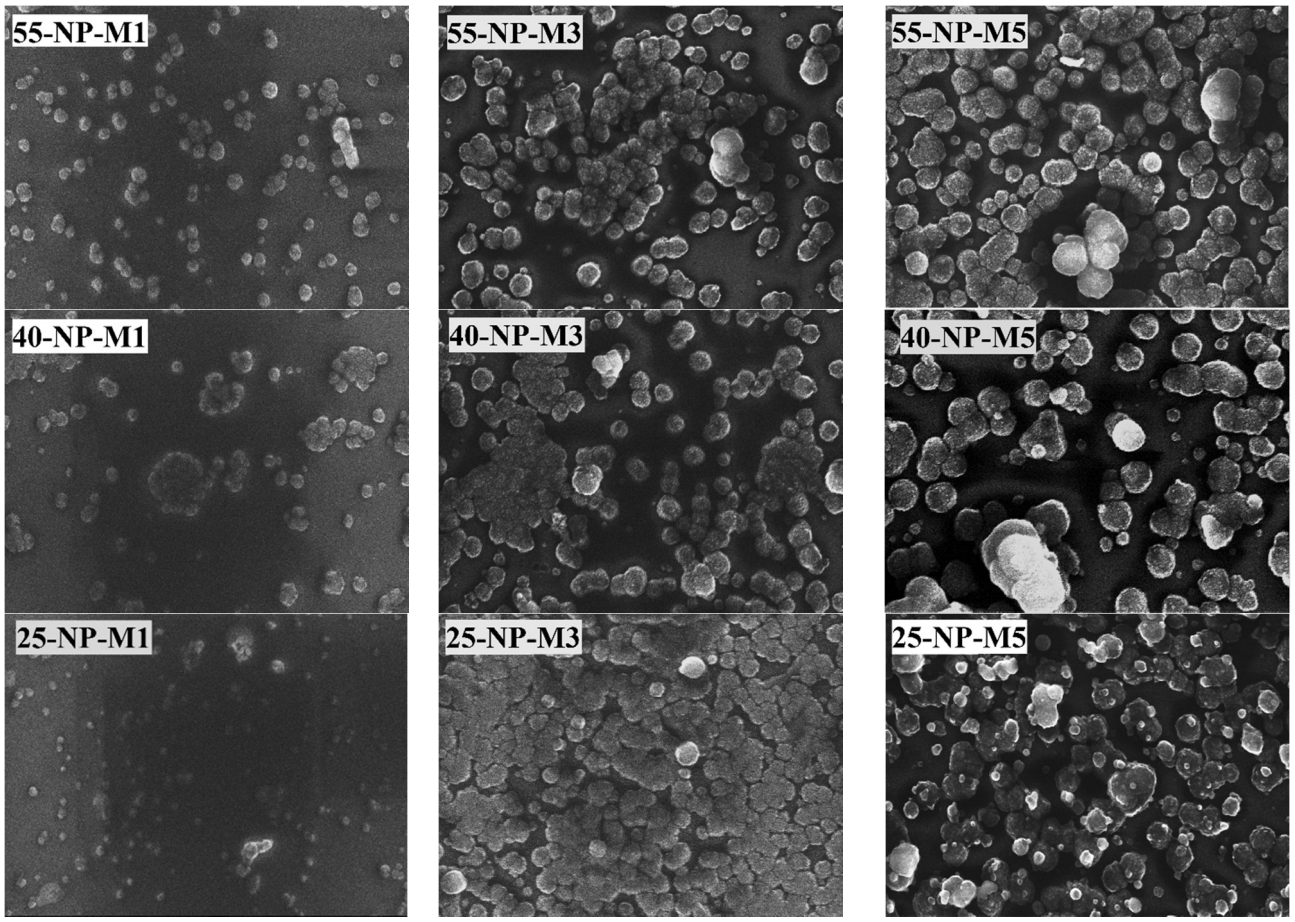

Figure 5.5. SEM images (50000x) of the samples surface with different deposited times obtained with non-proper thiourea concentration.

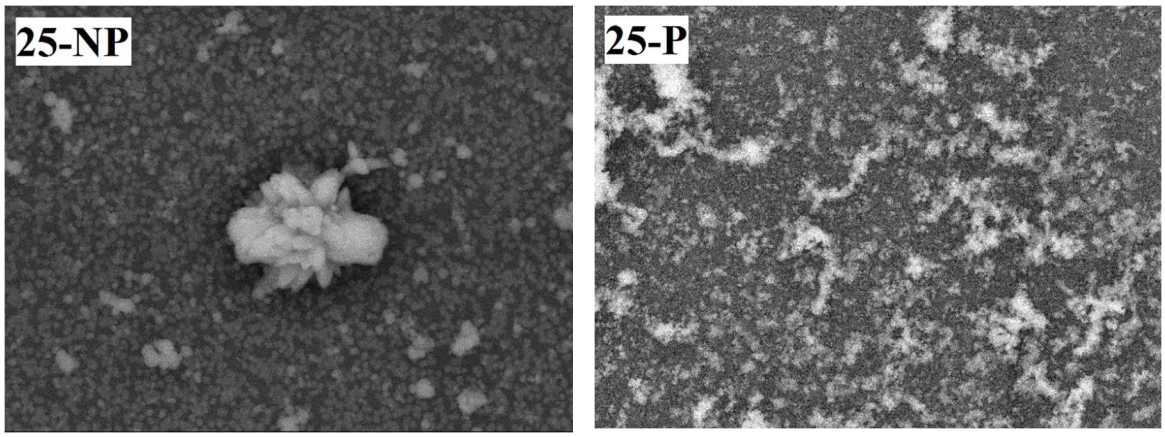

Figure 5.6. SEM images (10000x) of the surface of sample obtained at 25 °C with non-proper (25-NP) and with proper (25-P) thiourea concentrations.

5.4. Optical characterization

Figure 5.7 shows the optical transmittance spectra of all the samples for a wavelength range between 300 and 1100 nm.

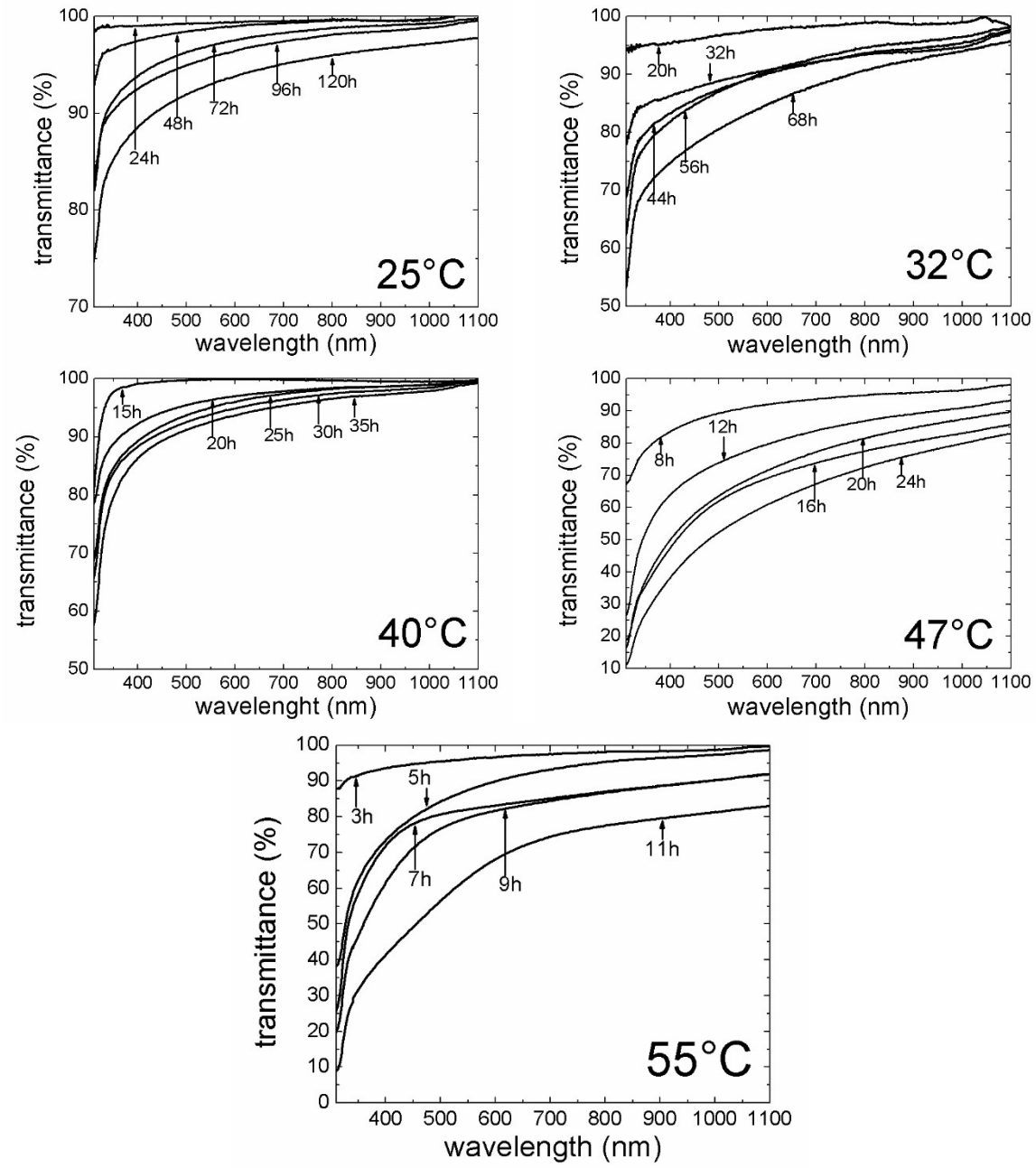

Figure 5.7. Optical transmittance spectra of the samples obtained with proper concentration of thiourea.

For all the temperatures, the samples show similar behavior with a high optical transmittance (greater than 80%) above 500 nm. As the deposition time increases, the transmittance of the sample is reduced due to the higher thickness and the better distribution of the grains on the surface of samples. Of all the samples, the only one with a better edge and higher optical transmittance, above 90%, is the sample prepared at 40 °C. The direct bandgap energy (E_g) of the ZnS films was measured by spectrophotometry technique and calculated from the absorption spectra through Eq. (3.1). Figure 5.8 shows the plot of α^2 vs energy of the incident photons. For all the temperatures, well-defined absorption edges are formed. An almost linear behavior of α^2 vs energy can be observed for all the samples, excepting for the samples with minor deposition time, i.e., minor thickness. The increase of α^2 value with time and temperature is explained by the higher thickness value reached of each sample. The E_g values measured on the ZnS films at different temperatures and deposition times are shown in the inset of Fig. 5.8. The E_g values ranged between 3.51 and 3.82 eV for all the samples. The reported bandgap energy value of the bulk-ZnS is 3.72 eV; in comparison, the estimated E_g values of the ZnS films are mainly closer to its bulk value. The slight differences with the bulk value may be due to the thickness of sample (high E_g values) or to the amount of oxygen contained in sample (low E_g values). Comparatively, the bandgap energy value reported for $Zn(OH)_2$ is ~3.06 eV [51]. Thus, the reduced E_g values measured on the deposited films can be explained in terms of the presence of the hydroxide compound.

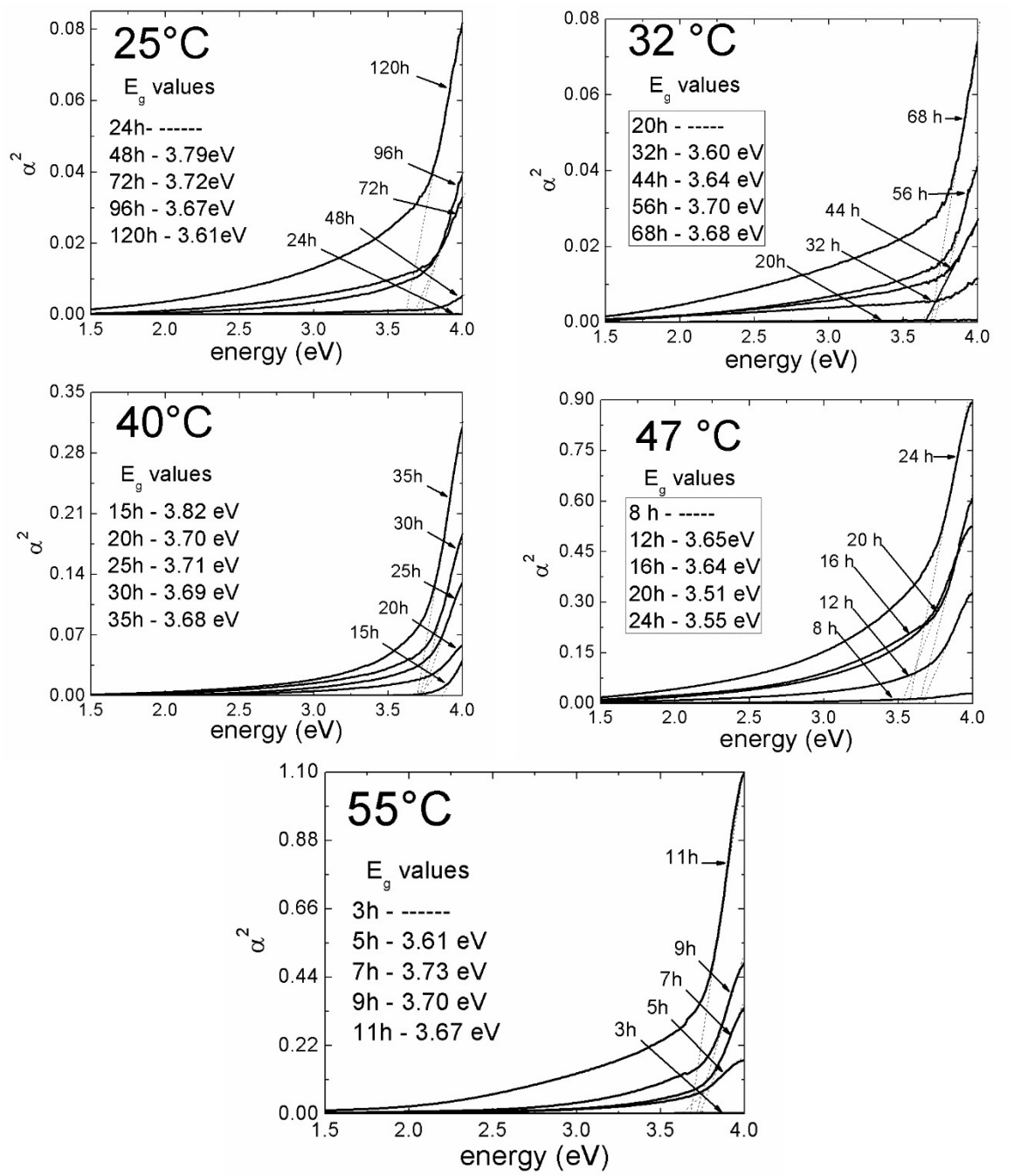

Figure 5.8. α^2 vs $h\nu$ plots of the ZnS samples deposited with different temperatures and proper conditions.

This effect is most noticeable for samples prepared under no proper thiourea concentrations as is shown in Figure 5.9. The first notable difference is the loss of the absorption edge which is not well defined. These samples present lower E_g values than those estimated with proper concentrations of thiourea and their values are below the bulk. These E_g values of samples, having the highest amount of oxygen, present an E_g modulation and can be related with the $Zn(OH)_2$ compound.

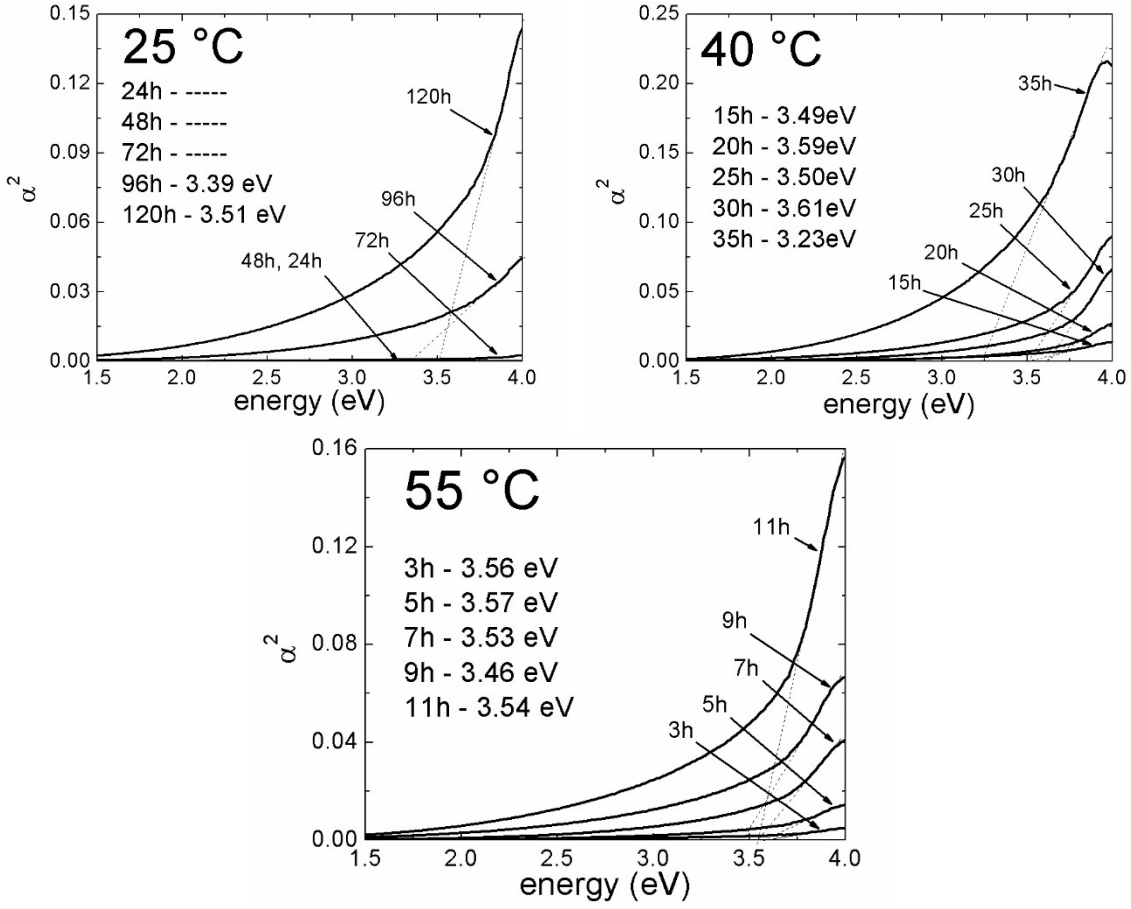

Figure 5.9. α^2 vs $h\nu$ plots of the ZnS samples deposited with different temperatures with non-proper thiourea conditions.

5.5. Proposal of the ZnS growth mechanisms at temperatures close to the ambient

According to the results obtained from the physicochemical, kinetic and characterization analysis, the growth mechanism that explains better our system is the *decomposition of a complex* mechanism since it implies elemental processes such as adsorption/chemisorption of species at superficial sites of the substrate and chemical reactions between adsorbed species (typical of processes with high values of energies of activation). Under this consideration, the following four steps are proposed for explaining the growth mechanism of the ZnS formation from temperatures between 25 °C and 55 °C:

Step 1. Formation of the complexing species of zinc in the growth solution:

$$Zn^{2+} + 3OH^- \rightarrow Zn(OH)_3^- \quad (5.1)$$

$$Zn^{2+} + 4OH^- \rightarrow Zn(OH)_4^{2-} \quad (5.2)$$

Step 2. Diffusion and adsorption of the complexing agent and $Zn(OH)_2$ formation on the surface of the substrate:

$$Zn(OH)_3^- + site \rightarrow Zn(OH)_{2(ads)} + OH^- \quad (5.3)$$

$$Zn(OH)_4^{2-} + site \rightarrow Zn(OH)_{2(ads)} + 2OH^- \quad (5.4)$$

Step 3. Decomposition of thiourea

$$SC(NH_2)_2 + OH^- \rightarrow HS^- + CN_2H_2 + H_2O \quad (5.5)$$

Step 4. Exchange reaction between OH^- and HS^- for ZnS formation:

$$Zn(OH)_{2(ads)} + HS^- \rightarrow ZnS_{(s)} + OH^- + H_2O \quad (5.6)$$

According to the results of the physicochemical analysis, the pH of the solution must be found in the zone of hydroxides in order to assure enough amounts of sulfur ions in the solution. For this reason, the complexing agents responsible for the growth of the material

are the $Zn(OH)_3^-$ and $Zn(OH)_4^{2-}$ hydroxy-complexes ions as is shown in Figure 4.5 (step 1). However, these two complex ions could not be the growth nuclei of ZnS because the silicon-based substrates have a preferential adsorption for neutral metal hydroxides such as $Zn(OH)_2$ [52]. From Figure 4.5 it can be observed that the $Zn(OH)_2$ complex does not exist as a predominant species in the range of pH measured during all the deposition time. Thus, it is necessary that the hydroxy-complexes are adsorbed on the substrate, forming $Zn(OH)_2$ by releasing OH^- ions on the surface of the substrate (step 2). Zinc hydroxide complex plays a very important role during the growth of ZnS by its role as a growth nucleus on which the formation of ZnS will take place. The sulfur specie, were determined with the HS^- predominant ions, and must be part of the ZnS growth process (step 3). In order to initiates the growth process, it is necessary to achieve a degree of supersaturation between the species [53], i.e., sufficient amounts of $Zn(OH)_2$ nuclei on the surface of the substrate, well as HS^- ions in the solution, thus, an exchange reaction between these two species could be carried out (step four).

The required time, for the system, to reach this degree of supersaturation is the *induction time* for the deposition. For higher temperatures of the solution, the thermal energy is provided to the major species ($Zn(OH)_3^-$ and $Zn(OH)_4^{2-}$ ions), such that the rate of formation of nuclei increases. On the other hand, the temperature promotes the hydrolysis of thiourea which leads to a large concentration of HS^- ions in the solution. These two factors can achieve supersaturation of the system by reducing the induction time and increasing the rate of growth for higher temperatures (55 °C, 47 °C, and 40 °C).

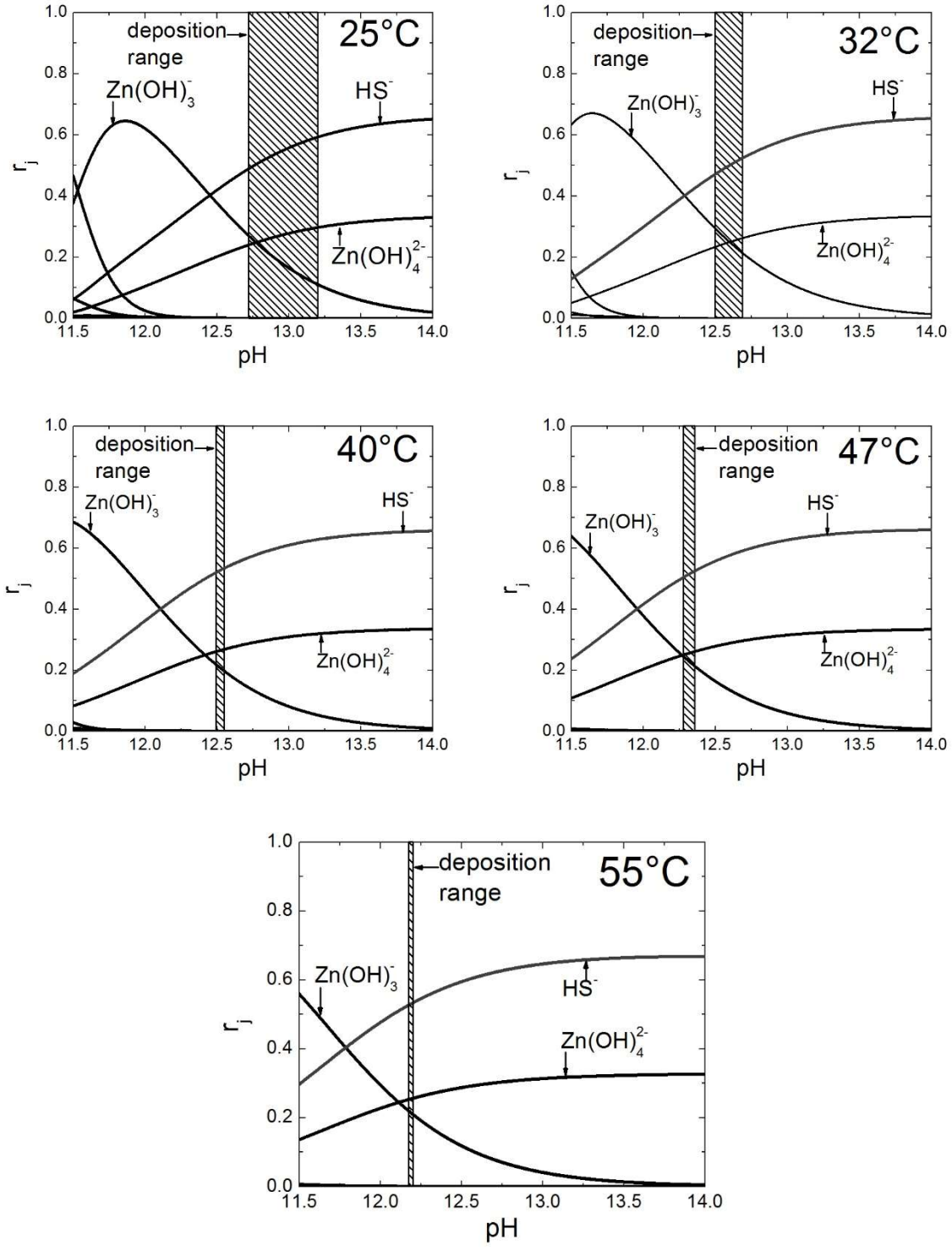

Figure 5.10. Species distributions diagrams obtained with proper conditions. The shaded areas represent the range of pH values measured in the solution.

Nevertheless, for temperatures near to the ambient (32 °C and 25 °C), the ions could remain passive causing a decrease in the HS^- ions and nuclei formation, and consequently, a delay in the onset of growth (larger induction times) and a decreased rate of growth of the material. However, the limiting factor in the growth of ZnS is the hydrolysis of the thiourea and not the growth nuclei formation, given the value of the order of the reaction. This fact can be clearly noted in films deposited under non-proper conditions. As only the concentration of thiourea is modified, both its dissociation and the rate of formation of the nuclei must remain unchanged for each temperature, which can be observed for similar induction times for proper and non-proper conditions. However, by reducing the amount of HS^- ions in the solution, the rate of growth of the material must be modified since the exchange reaction responsible for the ZnS growth could not be optimally carried out. Additionally, having low rates of growth, the maximum thickness of the material would decrease for the same reason. Similarly, since the HS^- ions are not spent in the solution, there exist a possibility that not all the $Zn(OH)_2$ nuclei will be converted to ZnS, whereby the thin film would have a double phase containing hydroxide and sulfide. This reasoning can explain the double slope observed in Fig. 4.2 for the sample grown at 25 °C with non-proper thiourea condition.

Finally, the proposed mechanism also explains the differences between the initial pH and the final pH values of the solution during deposition. Equations (5.1), (5.2), and (5.5) are considered as consumers of OH^- ions which cause a decrease in the pH of the solution; on the other hand, Eqs. (5.3), (5.4), and (5.6) are OH^- ions producers, with tendency to increase the pH of the solution. Experimentally, a tendency for reducing the pH value with time can be noted (Figure 4.3), such that consumers OH^- ions must be faster than producers OH^- ions.

When the pH value remains constant there exist a balance between production and consumption of OH^- ions. Since the limiting reaction is the hydrolysis of thiourea, Eq. (5.5) plays an important role in the variation of the pH value of the solution. If not enough OH^- ions are produced, an excess of $Zn(OH)_2$ nuclei can appear, which would generate a higher consumption of OH^- ions in the solution. If there is no exchange between the OH^- and the HS^- ions, the $Zn(OH)_2$ nuclei would solidify creating a double compound in the deposited film, known as Zn(S, OH) (Figure 5.1), and the pH of the solution must be decreased (non-proper conditions).

For films deposited under the proper conditions, this effect should be minimized since the changes of pH were not very noticeable, excepting for films deposited at 25 ° C, where larger variations in the pH of the solution was observed. Note that the greatest variation of pH at this reduced temperature mainly occurs in the induction phase, which is expected by the greater consumption of OH^- ions for the formation of the growth nuclei. However, then the pH value remains almost constant, in the growing zone, is indicative that the nucleation process is reduced or finished, and the formation of the film of ZnS begins, whereby Eqs. (5.5) and (5.6) would have similar rates of growth and therefore, the pH should not be modified. For films deposited under non-proper conditions, this factor is further accentuated given the lack of sufficient amount of HS- ions in the solution, and the reduction of the recombination of OH- ions, producing greater changes in the pH of the solution.

CONCLUSIONS

A physicochemical analysis was performed on the ZnS growth solution, from which the solubility curves and the species distribution diagrams of the material were obtained for temperatures between 25 °C and 55 °C. The solubility curves indicates the necessity to adjust the thiourea concentration according to the bath temperature used for the ZnS formation in order to contribute with enough amounts of sulfur ions in the bath solution. The most proper thiourea concentrations for the reported temperatures were 0.7 M (55 °C), 0.95 M (47 °C), 1.25 M (40 °C), 1.7 M (32 °C) and 2.25 (25 °C).

In the kinetic analysis the growth phases of the material for each temperature as well as the activation energy were determined. The measurements of thickness of the samples showed that thickness and the rate of growth increase with the increase of temperature. The estimated value of the activation energy of 127 ± 5 kJ/mol means that the growth mechanism of films is carried out by means of chemical interactions. The order of the reaction dependent on the concentration of thiourea was 1.03 ± 0.05, a value that confirms the dependence of the growth rate on the concentration of thiourea. According to the pH value and the species distribution diagrams, the deposition of the material was done in the hydroxide (pH > 11) region; therefore, the responsible of the growth of the material are the $Zn(OH)_3^-$ and $Zn(OH)_4^{2-}$ as zinc complexing ions, and HS^- as source of sulfur ions. From the set of these results a growth mechanism was proposed, which involves:

i. Adsorption of the hydroxide complex and formation of $Zn(OH)_2$ on the surface of substrate.
ii. Interchange reaction between HS^- and OH^- ions to form ZnS.

According to the proposed growth mechanism, thiourea concentrations lower than the proper values produce excess of zinc hydroxi-complexes into the solution, which produces a double phase between ZnS and $Zn(OH)_2$ leading to the formation of films with poor quality during deposition.

From characterization, the samples deposited with proper concentrations of tiourea presented better properties than for films deposited with non-proper conditions. The chemical characterization results by the XPS technique showed that, despite the proper concentration of thiourea, the exchange reaction between the ions is not carried out properly. At temperatures very close to the ambient, mixed compounds of ZnS and $Zn(OH)_2$ were found in the samples according to the value of the peak area ratio (ε) when the temperature is reduced. The temperature affects the conversion between the ions, therefore the stoichiometric molar ratio Zn/S increases from 0.367 at 25 °C to 0.906 at 55 °C whereby a better stoichiometry is obtained at slightly higher temperatures than the ambient temperature. This effect seems more noticeable when the samples are deposited with non-proper concentrations of thiourea, as they showed the lowest values of the stoichiometric ratio and peak area ratio as compared to their appropriate counterparts.

For the structural characterization, the samples deposited at 25 °C, a crystalline phase corresponding to the orthorhombic structure of $Zn(OH)_2$ was observed. The samples deposited at 32 °C and 40 °C showed an amorphous structure. For samples deposited at 47 °C and 55 °C a mainly structure corresponding to the orientation (111) of cubic structure (sphalerite) was obtained. The morphological characterization performed using the SEM technique showed that the samples grown with appropriate conditions display an evolution of the size of the grains according to the temperature of the solution. At 55 °C the surface of

the sample presents well-defined grains with spherical shape and larger size than the other samples obtained at lower temperatures.

Samples at 25 °C deposited with non-proper thiourea concentration showed bigger particles tube-like with thorns superimposed on the surface. A chemical analysis revealed the presence of zinc and oxygen atoms but not sulfur, confirming the considerations of the growth mechanism proposed. The optical characterization corroborated the behavior of the thickness of samples given the dependence of the later with the value of the absorption coefficient. The values of the bandgap energy of the samples were in a range from 3.5 to 3.8 eV for samples obtain with proper conditions. Otherwise, the samples synthesized with non-proper conditions showed lower values due to the impurities of $Zn(OH)_2$ found on the samples. The optical transmittance spectra on samples obtained with appropriate conditions can be used as optical window in solar cells of thin layer due to the higher than 80 % value of transmittance for wavelengths above 500 nm.

The samples deposited at 40 °C presented the most outstanding properties for solar cells applications because of their adequate average bandgap energy of 3.72 eV and optical transmittance above 80 % in the visible spectrum.

REFERENCES

[1] S. M. Pawar, B. S. Pawar, J. H. Kim, Oh-Shim Joo, C. D. Lokhande, *Curr. Appl. Phys*., **11**, 117 (2011).

[2] P. O'Brien, J. McAleese, *J. Mater. Chem*., **8**, 2309 (1998).

[3] R. S. Mane C. D. Lokhande, *Mater. Chem. Phys*., **65**, 1 (2001).

[4] J.A. García-Valenzuela, M.R. Baez-Gaxiola, M. Sotelo-Lerma, *Thin Solid Films,* **534**, 126 (2013)

[5] Yung-Tang Nien, In-Gann Chen, *J. Alloys. Comp.*, **471**, 553 (2009).

[6] C.D. Lokhande, Eun-Ho Lee, Kwang-Deog Jung, Oh-Shim Joo, *Mater. Chem. Phys*., **91,** 200 (2005).

[7] P. Jackson, D. Hariskos, E. Lotter, S. Paetel, R. Wuerz, R, Menner, W. Wischmann, W, M. Powalla, *Prog. Photovolt: Res. Appl*., **19,** 894 (2011).

[8] A.I. Oliva, O. Solís-Canto, R. Castro-Rodríguez, P. Quintana, *Thin Solid Films,* **516,** 5967 (2008).

[9] Qi Liu, Guobing Mao, *Surf. Rev. Lett.*, **16,** 469 (2009).

[10] M. A. Contreras, T. Nakada, M. Hongo, A. O. Pudov, J. R. Sites, "ZnO/ZnS(O,OH)/Cu(In,Ga)Se2/Mo solar cell with 18.6% efficiency", Proceedings of the 3rd World Conference on Photovoltaic Solar Energy Conversion, 11-18 May, Osaka, Japan (2003).

[11] X. Wang, H. Huang, B. Liang, Z. Liu, D. Chen, G. Shen, *CRC. Cr. Rev. Sol. State,* **38**, 57 (2007).

[12] Y. Kavanagh, M. J. Alam, D. C. Cameron, *Thin Solid Films*, **85**, 447 (2004).

[13] U. Gangopadhyay, K. Kim, D. Mangalaraj, J. Yi, *Appl. Surf. Sci*., **230**, 364 (2004).

[14] X. S. Fang, T. Zhai, U. K. Gautamb, L. Li, L. Wu, Y. Bando, D. Golberg, *Prog. Mater. Sci.,* **56,** 175 (2011).

[15] X. S. Fang, Y. Bando, D. Golberg, *J. Mater. Sci. Technol.,* **24,** 512 (2008).

[16] A. Abdel-Kader, F.J. Bryant, *J. Mater. Sci*., **21**, 3227 (1986).

[17] U. Gangopadhyay, K.Kim, S.K. Dhungel, H. Saha, J. Yi, *Adv. Optoelectron*. **2007,** 1 (2007).

[18] T. Nakada, M. Mizutani, *Jpn. J. Appl. Phys.,* **41,** 165 (2002).

[19] O.L. Arenas, M. T. S. Nair, P. K. Nair, *Semicond. Sci. Technol*., **12**, 1323 (1997).

[20] J.M. Doña, J. Herrero, *J. Electrochem. Soc.,* **141**, 205 (1994).

[21] B. Mokkili, M. Froment, D. Lincot, *J. Physique IV.,* **5**, C3-261 (1995).

[22] C. D. Lokhande, *Mater. Chem. Phys*. **21**, 1 (1991)

[23] S. Biswas, P. Pramanik, P. K. Basu, *Mater. Letter*, **4**, 81 (1986).

[24] C. Hubert, N. Naghavi, B. Canava, A. Etcheberry, D. Lincot, *Thin Solid Films,* **515**, 6032 (2007).

[25] S. Tec-Yam, J. Rojas, V. Rejón, A.I. Oliva, *Mater. Chem. Phys,.* **136,** 386 (2012).

[26] I.J. González-Panzo, P.E. Martín-Várguez, A.I. Oliva, *J. Electrochem. Soc.,* **161**, D181 (2014).

[27] Liu Qi, Guobing Mao, Jianping Ao, *Appl. Surf. Sci*., **254**, 5711 (2008)

[28] C. Hubert, N. Naghavi1, A. Etcheberry, O. Roussel1, D. Hariskos, M. Powalla, O. Kerrec, and D. Lincot, *Phys. Stat. Sol. (a),* **205**, 2335 (2008).

[29] W. Vallejo, M. Hurtado, G. Gordillo, *Electrochimica Acta,* **55**, 5610 (2010).

[30] I. J. González-Panzo, P. E. Martín-Várguez, A. I. Oliva, *J. Electrochem. Soc*., **161**, D761 (2014).

[31] G. Hodes, *Chemical Solution Deposition of Semiconductors Films*, Marcel Dekker Inc, United States of America (2002).

[32] C.A. Rodríguez, M.G. Sandoval-Paz, G. Cabello, M. Flores, H. Fernández, C. Carrasco, *Mater. Res. Bull.,* **60**, 313 (2014).

[33] T. V. Vinogradova, V. F. Markov, L. N. Maskaeva, *Russ. J. Gen. Chem.,* **80**, 2341 (2010).

[34] A. I. Oliva-Avilés, R. Patiño, A. I. Oliva, *Appl. Surf. Sci*., **256,** 6090 (2010).

[35] S. D. Sartale, B. R. Sancapal, M. Lux-Steiner, A. Ennaoui, *Thin Solid Films,* **480-481,** 168 (2005).

[36] J. Cheng, D. B. Fang, H. Wang, B. W. Liu, Y. C. Zhang, H. Yan, *Semicond. Sci. Technol.,* **18,** 676 (2003)

[37] Atkins De Paula, *Química Física*, Ed. Médica Panamericana, (2008).

[38] P. Uday Bhaskar, G. Suresh Babu, Y.B. Kishore Kumar, Y. Jayasree, V. Sundara Raja, *Mater. Chem. Phys.,* **134,** 1106 (2012).

[39] Huan Ke, Shuwang Duo, Tingzhi Liu, Qi Sun, Chengxiang Ruan, Xiaoyan Fei, Jilin Tan, Sheng Zhan, *Mater. Sci. Semicond. Process,* **18,** 28 (2014)

[40] M. Reinisch, C.L. Perkins, K.X. Steirer, *ECS J. Solid State Sci. Technol.* **5**, P58 (2016).

[41] Sambhu Kundu, Larry C. Olsen, *Thin Solid Films,* **471,** 298 (2005)

[42] P. Roy, J. R. Ota, S. K. Srivastava, *Thin Solid Films,* **515,** 1912 (2006)

[43] K. Deepa, K.C. Preetha, K.V. Murali, A.C. Dhanya, A.J. Ragina, T.L. Remadevi, *Optik*¸ **125**, 5727 (2014)

[44] R. Ortega-Borges, D. Lincot, *J. Electrochem. Soc*., **140**, 3464 (1993).

[45] J.F. Moulder, W.F. Stickle, P.E. Sobol, K.D. Bomben, *Handbook of X-ray Photoelectron Spectroscopy*, Perkin-Elmer Corporation, United States of America (1992)

[46] Y-C. Ling, Y-T. Chao, P-C. Yao, *Appl. Surf. Sci.,* **307**, 724 (2014).

[47] K. Ahn, J. H. Jeon, S. Y. Jeong, J. M. Kim, H. S. Ahn, J. P. Kim, E. D. Jeong, C. R. Cho, *Curr. Appl. Phys.,* **12,** 1465 (2012)

[48] D.A. Johnston, M.H. Carletto, K.T.R. Reddy, I. Forbes, R.W. Miles, *Thin Solid Films*, **403-404**, 102 (2002)

[49] G. Liang, P. Fan, C. Chen, J. Luo, J. Zhao, D. Zhang, *J. Mater. Sci. Mater. Electron.,* **26**, 2230 (2015).

[50] R. Sahraei, G. Motedayen Aval, A. Baghizadeh, M. Lamehi-Rachti, A. Goudarzi, M. H. Majles Ara, *Mater. Lett.,* **62,** 4345 (2008)

[51] Z. Islam, T. Gayen, M. Seredych, O. Mabayoje, L. Shi, T.J. Bandosz, R.R. Alfano*, J. Appl. Phys.,* **114**, 043522 (2013).

[52] P. C. Rieke, S. B. Bentjen, *Chem. Mater*., **5**, 43 (1993)

[53] X. S. Fang, Y. Bando, M. Liao, U.K. Gautam, Ch. Zhi, B. Dierre, B. Liu, T. Zhai, T Sekiguchi, Y. Koide, D. Golberg. *Adv. Mater.,* 21 (2009) 2034-2039.

APPENDIX A. Scientific publications and works presented at congresses

- Publications.

  I. **I. J. González-Chan**, A.I. Oliva, Physicochemical analysis and characterization of chemical bath deposited ZnS films at near ambient temperature**.** *J. Electrochem. Soc.*, **163**, D421 (2016).

  II. A.I. Oliva, P.E. Martin-Várguez, I. J. González-Panzo, **I. J. González-Chan**. "Papel del diagrama de distribución de especies en la preparación de semiconductores por baño químico". *Rev. Mex. Ing. Quim*., **15**, 209 (2016).

  III. **I. J. González-Chan**, A.I. Oliva, Synthesis of ZnS thin films by chemical bath: from room temperature to 90°C**.** *J. Electrochem. Soc.*, **164**, D95 (2017).

- Congresses

  I. **I.J. González-Chan**, J.E. Corona, A.I. Oliva. "Efecto del $ZnSO_4$ en la preparación por baño químico del semiconductor ZnS". Memorias del *XIV Congreso Nacional de Ingeniería Eléctrica y Electrónica del Mayab (CONIEEM-2014)* Abril de 2014. Mérida Yucatán México. Págs. 353-359.

  II. **I.J. González-Chan**, A.I. Oliva. **"**Depósito y caracterización de capas delgadas de ZnS a temperatura ambiente". *LVIII Congreso Nacional del Física*, Octubre 05-09, 2015, Mérida, Yucatán, México.

  III. **I.J. González-Chan**, A.I. Oliva. "Chemical bath deposited ZnS films near room temperature: physicochemical considerations". Nanotechnology ID 9

(Materials and Applications). *13th International Conference on Electrical Engineering, Computing Science and Automatic Control*, September 26-30, 2016, Ciudad de México, México.

IV. **I.J. González-Chan**, A.I. Oliva. "Physicochemistry of the chemical bath deposited ZnS films near room temperature". Abstract 584. (TF-TuP20). *Pacific Rim Symposium on Surfaces, Coatings and Interfaces*, December 11-15, 2016, Hawaii, United States of America.

APPENDIX B. Future works

1. To investigate the effects of different concentrations of $ZnCl_2$, KOH and NH_4NO_3 on the properties of the CBD-ZnS films.
2. To continue the development of the kinetics to improve the law growth rate on the analysis of the growth mechanism of the ZnS.
3. To analyze the changes in the properties of the ZnS thin films and the chemical solution by using other type of substrates.